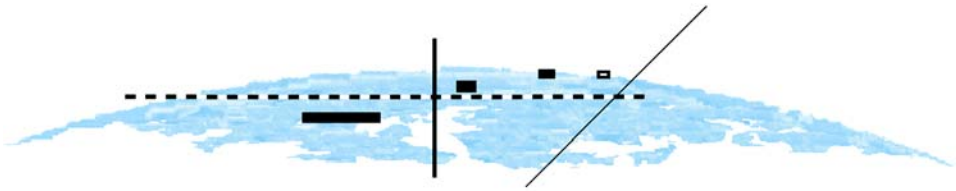

GeoForschungsZentrum Potsdam

STIFTUNG DES ÖFFENTLICHEN RECHTS

Scientific Technical Report

ISSN 1610-0956

Joachim Höpfner

Low-frequency variations, Chandler and annual wobbles of polar motion as observed over one century

Scientific Technical Report STR03/01

Low-frequency variations, Chandler and annual wobbles of polar motion as observed over one century

Joachim Höpfner

GeoForschungsZentrum Potsdam, Division 1: Kinematics and Dynamics of the Earth,Telegrafenberg, D-14473 Potsdam, Germany; E-mail: ho@gfz-potsdam.de

Abstract. Polar motion data is available from the mid-19th century to the present. Based on time series with a variety of sampling intervals (monthly, 0.05-year, 5-day and daily), we have separated the low-frequency terms by low-pass filtering and the Chandler and annual terms by recursive band-pass filtering of the pole coordinates. Using a simple unweighted least-squares fit to the filtered low-frequency terms, the linear trends of the rotation pole were estimated. Assessing the estimates based on intercomparisons, the most reliable trend estimate was found. Using a Fast Fourier Transform, we have computed the prograde, retrograde and total amplitude spectra of the low-frequency part of polar motion in order to reveal the long-periodic signals. The characteristics and time evolution of the Chandler and annual wobbles are described by changes in their parameters (radii, directions and period lengths) over one century.

Key words: Polar motion, main components, low-frequency variations (secular drift, long-periodic signals), Chandler wobble, annual wobble, parameter (radius, direction, period length), variability, cycles

1 Introduction and objective

Relative to the rotating, terrestrial body-fixed reference frame, variations in the Earth's rotation are measured by polar motion (PM) and changes in the length-of-day (LOD). To study Earth rotation, optical astrometry was used since the beginning of such studies in the mid-19th century until about 1980. Since the middle of the 1970s, precise space geodesy techniques such as VLBI (Very Long Baseline radio Interferometry), LLR (Lunar Laser Ranging), SLR (Satellite Laser Ranging) have been used, while from 1992 GPS (Global Positioning System) and DORIS (Doppler Orbit determination and Radiopositioning Integrated on Satellite) have come into use for determining the temporal variations in the Earth orientation parameters (EOPs). These studies are associated with the work of the International Latitude Service (ILS), the International Polar Motion Service (IPMS) and the Bureau International de l'Heure (BIH), and then the International Earth Rotation Service (IERS). For more information, see Dick et al. (2000) and Höpfner (2000) and the references therein.

The intensive efforts that have gone into the study of Earth rotation mean that polar motion data is available from the mid-19th century to the present. For the period 1846-1890, the PM solutions derived by Rikhlova (see Fedorov et al. 1972) are based on three series of absolute declination observations at Pulkovo, Greenwich, and Washington. From about 1890-1900, astronomical latitude observations from 20 independent stations became available. Over the next 80 years, the ILS and from 1962 the IPMS provided systematic and continuous latitude observations from ILS/IPMS stations. Other latitude measurements were made with different types of instruments (astrolabes, photographic zenith tubes and visual zenith telescopes) at independent stations on the Northern and Southern hemispheres, in particular from 1955 when the BIH, hosted by the Paris Observatory (and operating from 1919), installed its own polar motion service denoted as Service International Rapide des Latitudes (SIR), and more intensivly from 1957 at the beginning the International Geophysical Year (IGY). Based on measurements of the EOPs by optical astrometry, there are a number of PM solutions in terms of ILS and non-ILS time series. A review of these PM time series can be found in Höpfner (2000) and the references therein.

Compared to the combined Earth orientation series based on the precise space-geodetic measurements, the earlier PM data have a lower accuracy and temporal resolution. In the past however, it was the only available source of information

about the Earth's rotation pole. Therefore, because the PM time series obtained from past latitude observations are available over a much longer period than those taken by the modern space geodesy techniques, they are important for the study of the dominant components of PM, namely the secular drift and low-frequency motions and the Chandler and annual wobbles. Some information on the recent studies dealt with them should be noted.

Based on the longest astrometric series of pole coordinates determined by the Main Astronomical Observatory in Kiev (see Fedorov et al. 1972, and, e.g. IERS 2000), Nastula et al. (1993) studied the amplitude variations of the Chandler and annual wobbles of polar motion between 1846-1988. Using a variety of PM time series derived from optical and space geodetic data over various periods, Vicente and Wilson (1997) dealt with the variability of the Chandler frequency. Vondrák et al. (1998) and Vondrák (1999) used the Earth rotation parameters from 1899.7-1992.0, obtained from a reanalysis within the Hipparcos frame, to study the long-periodic polar motion, in particular the mean pole position, its drift and parameters of annual and Chandler wobbles, and applied a least-squares fit at running intervals of 8.5 years. Gross and Vondrák (1999) estimated the trend in the pole path from the Hipparcos polar motion series, the homogeneous ILS series and the SPACE96 series and compared their estimates with other recent trend estimates. Liu et al. (2000) developed a new wavelet analysis technique and used it in order to quantify the period and amplitude of the Chandler wobble for the period 1900-1990. This method was also applied to detect the instantaneous amplitude and period of the annual oscillation. Based on two long PM time series, the EOP(IERS)C01 series and the Hipparcos series (labelled here OA97), Schuh et al. (2000, 2001) studied the linear drift of the pole, decadal variations and the Chandler and annual wobbles. In particular, a sliding 13.76-year window analysis in terms of a least-squares fit was used to determine the Chandler and annual wobble parameters. Using five PM time series, Vicente and Wilson (2002) examined the long-period polar motion with respect to what portion represents true polar motion.

The state of the art in studying polar motion in the past is the character of the long-periodic variations, which still remain uncertain. Therefore, and motivated by the higher temporal resolution of the Hipparcos polar motion series (the longest homogeneous PM series, with 5-day sampling, Vondrák et al. 1998), the problem is re-examined. The purpose of this paper is to present and discuss more precise estimates of the parameters of the major components of PM in their temporal variability covering the 20th century.

2 Polar motion data used in this study

For the period covering the mid-19th century to the present day, there are several homogeneous PM time series, distinguished by a variety of sampling intervals. In order to investigate the low-frequency terms and the Chandler and annual wobbles of polar motion, the following PM time series are used:

- POLE2001(JPL), a combined Earth orientation series with monthly sampling available from the JPL (Jet Propulsion Laboratory)
To form POLE2001, the homogeneous ILS series computed from the reanalysis of the ILS latitude observations in a consistent way for the period 1899.9–1979.0 at monthly intervals by Yumi and Yokoyama (1980) has been combined with COMB2001. To produce COMB2001, the BIH optical astrometric series determined by Li (1985, also see Li and Feissel, 1986) was combined with SPACE2001. The standard errors of polar motion are about 20 mas for the x-component and about 16 mas for the y-component between 1900 to 1962. They are estimated to be gradually decreasing from about 9 to 0.1 mas during 1962 to 2001. For more information on the combination of Earth orientation measurements to SPACE2001, COMB2001, and POLE2001, see, e.g., Gross (2000).

- EOP(IERS)C01, a combined Earth orientation series. Between 1846 to 1890 it has a 0.1-year sampling interval, and after this a 0.05-year interval. It is available from the IERS.
This time series is obtained by concatenating the following solutions: The solution for the period 1846-1899 derived from three series of absolute declination observations (Pulkovo, Greenwhich, Washington) by Rikhlova (see Fedorov et al. 1976), that for the period 1900-1961 derived from optical astrometry analyses based on the Hipparcos reference frame by Vondrák et al. (1995), the BIH and IERS solutions for the period 1962-1979, introducing Earth orientation measurements taken by space-geodetic techniques from 1969, and, based on space-geodetic techniques, the IERS solution for the period 1980 to the present (see, e.g., IERS 2000). Its uncertainty has dramatically improved from 100 mas in 1846 to about 0.2 mas today. A summary of the contributions of observational techniques to Earth rotation monitoring, and the evolution of the increased precision obtained since 1846 can be found in Gambis (2000).

- OA00(AICAS), a combined Earth orientation series with 5-day sampling available from the IERS
The OA00 (Optical Astrometry 2000) solution is obtained from the reanalysis of the latitude and universal time observations based on optical astrometry in the Hipparcos frame at the Astronomical Institute of Academy of Sciences of the

Czech Republic (AICAS) in Prague. During the first half of the 20th century, the standard errors are relatively stable and of the order of 30 mas. They later decrease to a minimum of about 10 mas in 1980–1985, after which they again slightly increase. See, e.g., Vondrák et al. (1995, 1998), Vondrák (1999); Vondrák and Ron (2000).

- EOP(IERS)C04, a combined Earth orientation series with one-day sampling available from the IERS
This IERS solution is currently recomputed to take advantage of the improvement in the various individual contributions, and of the refinement of analysis procedures. It is slightly smoothed by a Vondrak algorithm to remove the high-frequency noise. Note that the uncertainty of one daily value for the time series improves from 30 to 0.2 mas by replacing the classical method of measuring polar motion by space-geodetic techniques over time. See, e.g., IERS (2000).

- SPACE2001(JPL), a combined Earth orientation series with one-day sampling available from the JPL
This series begins in 1976 and only uses independent space-geodetic measurements of the Earth's orientation. Here, the estimated uncertainty of a daily value for both components of polar motion decreases from about 3 to 0.1 mas. See, e.g., Gross (2000).

Table 1. Characteristics of the various PM time series used in this work

PM time series	Entire time span in calendar time	Time interval in MJD	Sampling interval	Number of values	Reference
POLE2001(JPL)	1900 Jan. 20.7 ... 2001 Dec. 21.7	15039.674 ... 52264.736	30.4375 days	1224	Gross (2000)
EOP(IERS)C01	1890.00 ... 2000.00	11368.00 ... 51544.00	0.05 years	2201	IERS (2001)
OA00(AICAS)	1899 Sept. 25.405 ... 1991 Dec. 29.331	14922.405 ... 48619.331	5.034652 days	6693	Vondrák et al. (1998)
EOP(IERS)C04	1962 Jan. 1 ... 2002 May 9	37665.00 ... 52403.00	1 day	14739	IERS (2001)
SPACE2001(JPL)	1976 Sept. 28.0 ... 2002 Jan. 19.0	43049.00 ... 52293.00	1 day	9245	Gross (2000)

Concerning the pole coordinates x, y, note that in this study we use the mathematical coordinate system with x_1 = x and x_2 = -y, where the x_1-axis points towards the Greenwich Meridian and the x_2-axis towards the 90° East longitude. Table 1 summarizes the characteristics of the PM time series including the associated time intervals in calendar time and in Modified Julian Date (MJD).

3 Data processing and results

Filtering necessary to separate the variable signals from equidistant time series when studying their behaviour over time. Therefore, all the PM time series with various time sampling intervals are processed using suitable filters in an analogous way. In particular, we separate the low-frequency terms by low-pass filtering and the Chandler and annual terms by recursive band-pass filtering of the pole coordinates. For this purpose, the low-pass, Chandler and annual filters designed for one-day sampling (e.g., Höpfner 2001a, 2002a) are applied to the EOP(IERS)C04 and SPACE2001(JPL) time series.

For separating the low-frequency, Chandler and annual terms from the monthly POLE2001(JPL) values, the 0.05-year EOP(IERS)C01 values and the 5-day OA00(AICAS) values, the corresponding filters were still designed. For comparison, the characteristics of the digital filters used are given in Table 2. Moreover, the amplitude characteristics of the filters, that are computed as response functions of period length for each filter in terms of the ratio of the amplitude of the variations after filtering to that before, are shown in Fig. 1 (with logarithmic scaling in x).

When panels (a) to (d) of Fig. 1 are compared with each other, a good agreement between the response functions for analogous filters in their courses are seen. However, in each picture, the response functions of the Chandler and annual filters partially cover each other. Therefore, to derive optimal solutions for the Chandler and annual wobbles, we make use of recursive band-pass filtering. The procedure applied used the successive approximation by alternate elimination of the terms. However, using recursive band-pass filtering to separate the Chandler and annual terms from the PM time series requires estimates at the beginning and end of the resulting time series, which may be less accurate because of an edge effect (Höpfner 2002a).

The low-frequency, Chandler and annual terms filtered out from the PM time series were obtained as separate polar motions in the x_1- and x_2-components at the available sampling intervals. Table 3 presents the time intervals of the three resulting components, given in calendar time and MJD, and the data number in each filtered time series. Figure 2 shows the low-frequency terms filtered out from the POLE2001(JPL), EOP(IERS)C01, and OA00(AICAS) time series, with those for the x_1-component in the upper part and those for the x_2-component in the lower part. The same is shown

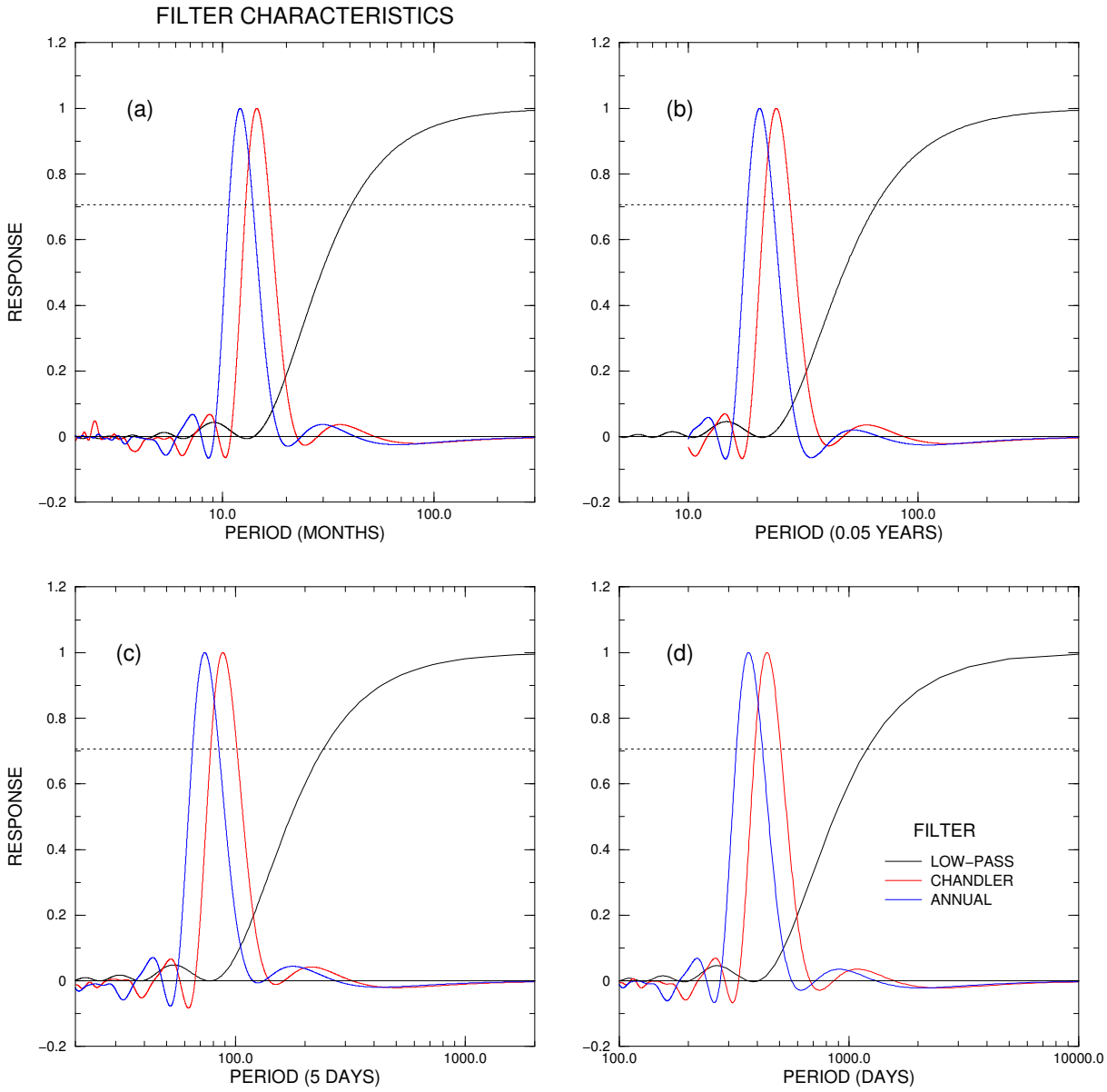

Figure 1. Amplitude characteristics of the filters used to separate the long-frequency component and the Chandler and annual oscillations from the original time series: (a) at monthly intervals, (b) at 0.05-year intervals, (c) at 5-day intervals and (d) at one-day intervals. The response is given as a function of period. Half-power points are the points of intersection between the individual curves and the horizontal light dotted line.

Table 2. Characteristics of the digital filters

Filter: Component	Period in sampling intervals	Number of points used in each filtering	Related edge effect: Points lost at either end	(a) Cut-off period (b) Half-power points of the filter
(a) used for monthly sampling				
Low-pass: Low-frequency		25	12	(a) 14; (b) 41
Band-pass: Chandler	14.51	63	31	(b) 13 and 17
Annual	12.10	53	26	(b) 11 and 14
(b) used for 0.05-year sampling				
Low-pass: Low-frequency		41	20	(a) 22; (b) 66
Band-pass: Chandler	24.18	105	52	(b) 21 and 28
Annual	20.45	89	44	(b) 18 and 23
(c) used for 5-day sampling				
Low-pass: Low-frequency		147	73	(a) 77; (b) 238
Band-pass: Chandler	87.95	381	190	(b) 78 and 101
Annual	73.37	317	158	(b) 65 and 85
(d) used for one-day sampling				
Low-pass: Low-frequency		731	365	(a) 415; (b) 1206
Band-pass: Chandler	440.53	1911	955	(b) 390 and 506
Annual	366.30	1589	794	(b) 324 and 421

Table 3. Time intervals of the main components filtered out from the PM time series given in calendar time and MJD and the data number in each filtered time series

(a) Time intervals in calendar time

PM time series	Low-frequency terms Time interval	Chandler terms Time interval	Annual terms Time interval
POLE2001(JPL)	1901 Jan. 20.924 ... 2000 Dec. 21.486	1902 Aug. 22.236 ... 1999 May 23.174	1902 March 23.049 ... 1999 Oct. 22.361
EOP(IERS)C01	1891.00 ... 1999.00	1892.60 ... 1997.40	1892.20 ... 1997.80
OA00(AICAS)	1900 Oct. 22.707 ... 1990 Dec. 29.800	1902 May 30.953 ... 1989 May 23.750	1901 Dec. 21.947 ... 1989 Oct. 30.747
EOP(IERS)C04	1963 Jan. 1 ... 2001 May 9	1964 Aug.13 ... 1999 Sept. 27	1964 March 5 ... 2000 March 6
SPACE2001(JPL)	1977 Sept. 28 ... 2001 Jan. 19	1979 May 11 ... 1999 June 9	1978 Dec. 1 ... 1999 Nov. 17

(b) Time intervals in MJD

PM time series	Low-frequency terms		Chandler terms		Annual terms	
	Time interval	Number of values	Time interval	Number of values	Time interval	Number of values
POLE2001(JPL)	15404.924 ... 51899.486	1200	15983.236 ... 51321.174	1162	15831.049 ... 51473.361	1172
EOP(IERS)C01	11733.00 ... 51179.00	2161	12317.00 ... 50594.00	2097	12171.00 ... 50740.00	2113
OA00(AICAS)	15314.707 ... 48254.800	6547	15899.953 ... 47669.750	6313	15739.947 ... 47829.747	6377
EOP(IERS)C04	38030.00 ... 52038.00	14009	38620.00 ... 51448.00	12829	38459.00 ... 51609.00	13151
SPACE2001(JPL)	43414.00 ... 51928.00	8515	44004.00 ... 51338.00	7335	43843.00 ... 51499.00	7657

Table 4. Linear trend rates of the rotation pole derived from the PM time series

PM time series	x_1-component	x_2-component	Linear trend rate	
			Magnitude	Direction
	mas/year	mas/year	mas/year	^{o} West
POLE2001(JPL)	1.180 ± 0.020	-3.326 ± 0.019	3.530 ± 0.019	70.46 ± 0.32
EOP(IERS)C01	1.639 ± 0.013	-3.541 ± 0.023	3.901 ± 0.022	65.17 ± 0.22
OA00(AICAS)	1.139 ± 0.009	-1.940 ± 0.010	2.250 ± 0.010	59.58 ± 0.24
EOP(IERS)C04	1.637 ± 0.007	-4.249 ± 0.008	4.554 ± 0.008	68.93 ± 0.09
SPACE2001(JPL)	0.525 ± 0.010	-3.482 ± 0.014	3.521 ± 0.014	81.42 ± 0.17

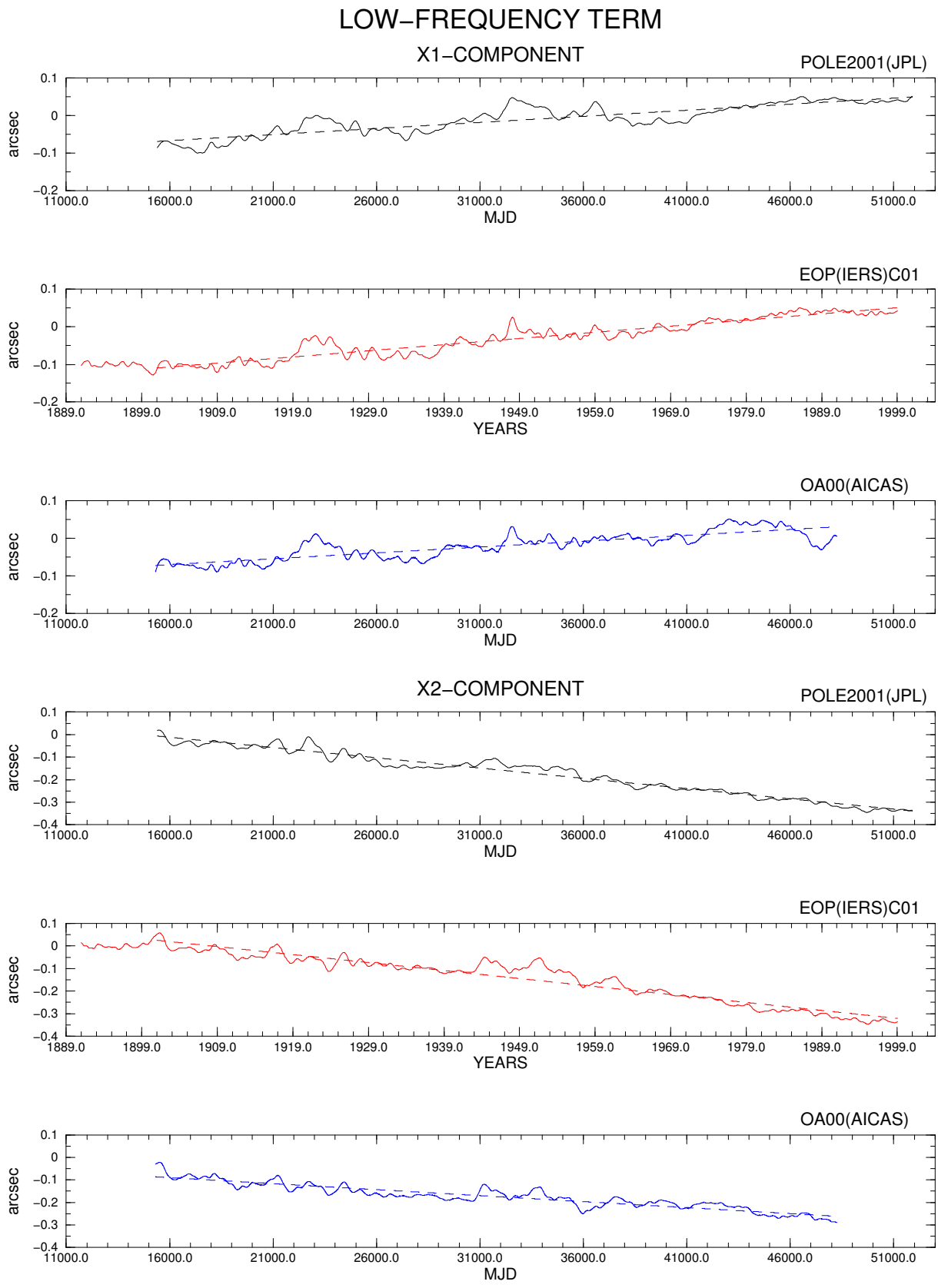

Figure 2. The low-frequency term of polar motion in the x_1-component (upper part) and the x_2-component (lower part). For each part, the motions shown are filtered out from the POLE2001(JPL) (top), EOP(IERS)C01 (centre), and OA00(AICAS) time series (bottom). Linear trends are indicated as dashed lines.

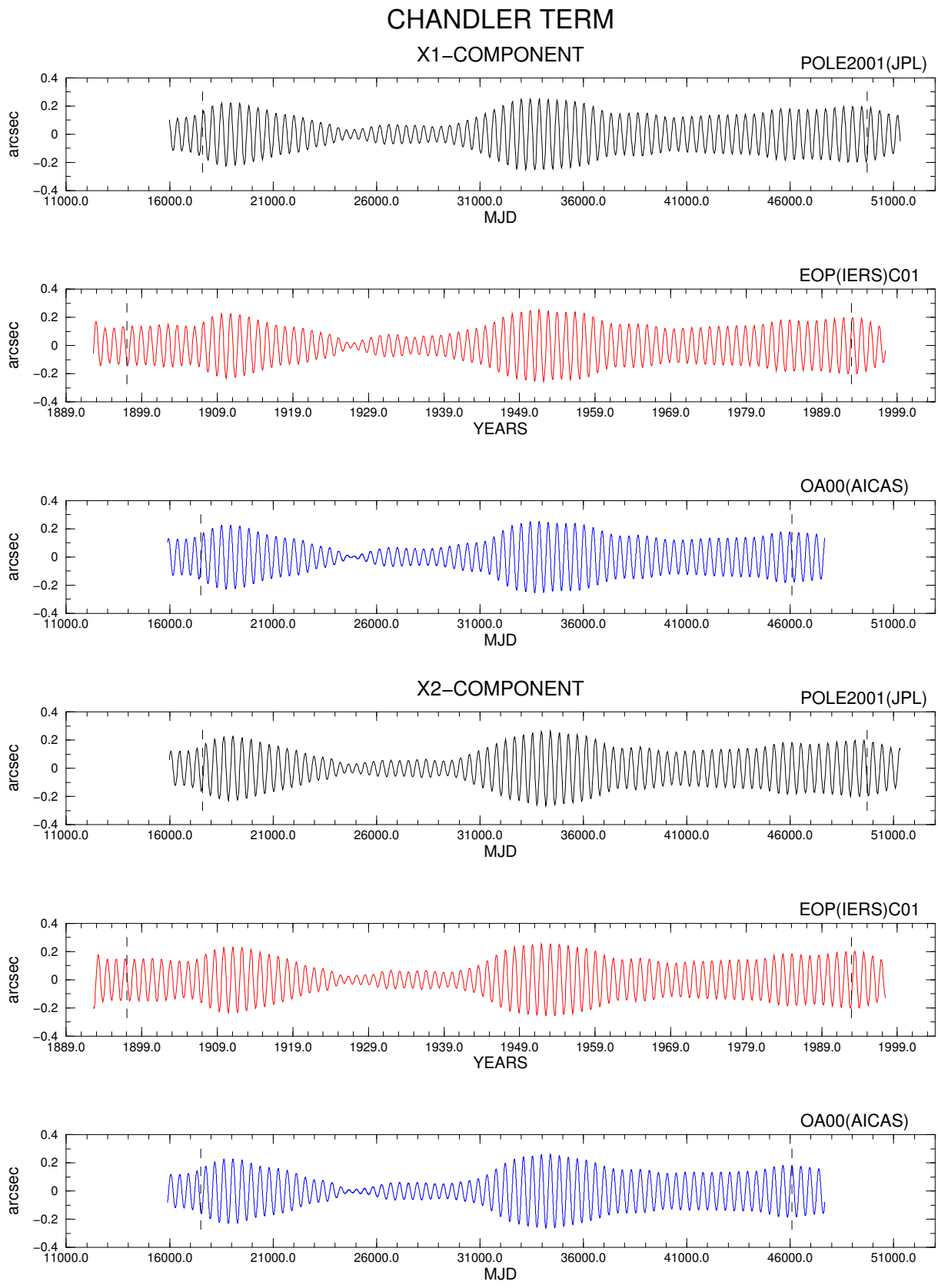

Figure 3. The Chandler term of polar motion in the x_1-component (upper part) and the x_2-component (lower part). For each part, the motions shown are filtered out from the POLE2001(JPL) (top), EOP(IERS)C01 (centre), and OA00(AICAS) time series (bottom). The time limits for the edge effects are indicated as dashed lines.

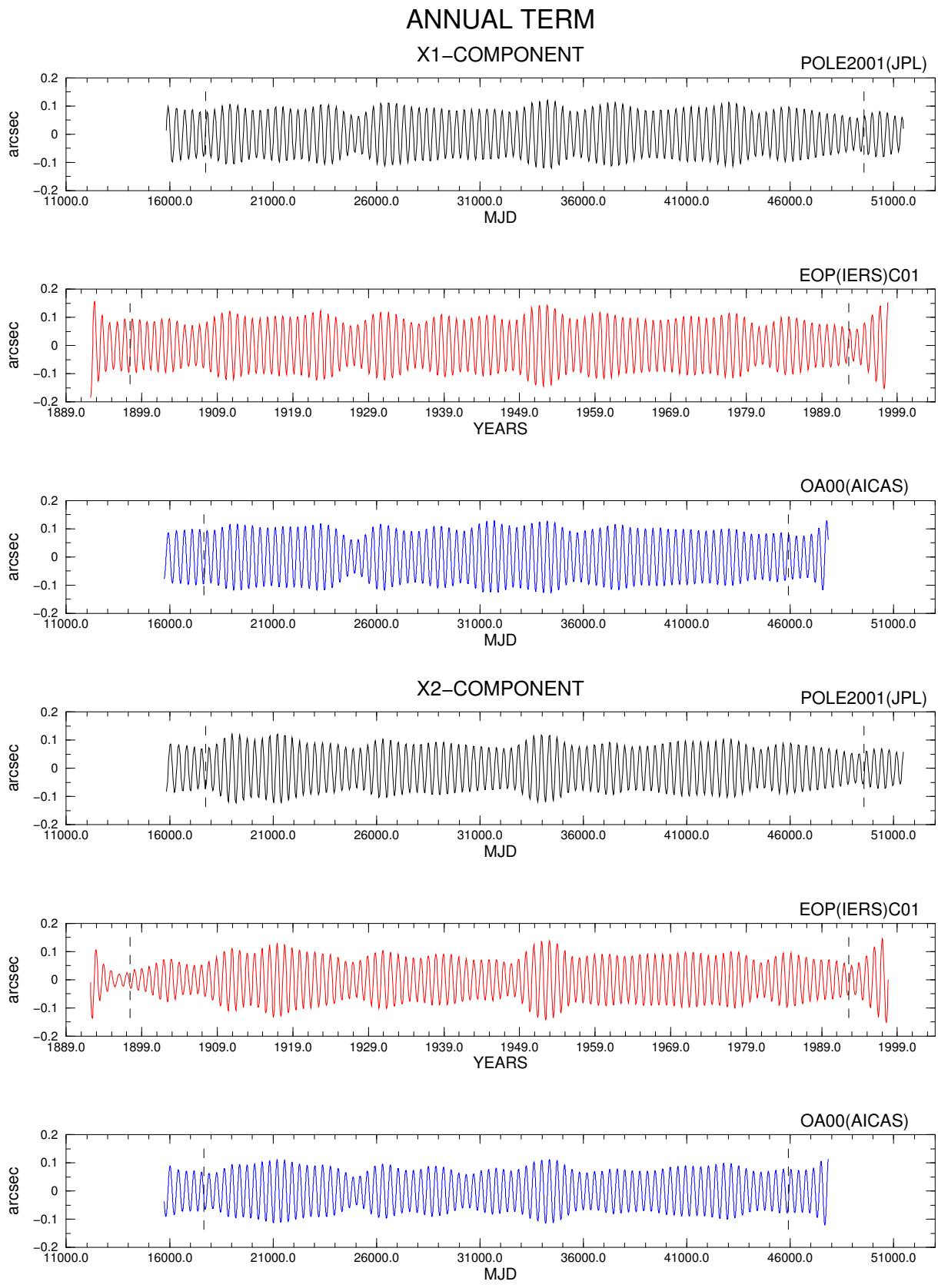

Figure 4. The annual term of polar motion in the x_1-component (upper part) and the x_2-component (lower part). For each part, the motions shown are filtered out from the POLE2001(JPL) (top), EOP(IERS)C01 (centre), and OA00(AICAS) time series (bottom). The time limits for the edge effects are indicated as dashed lines.

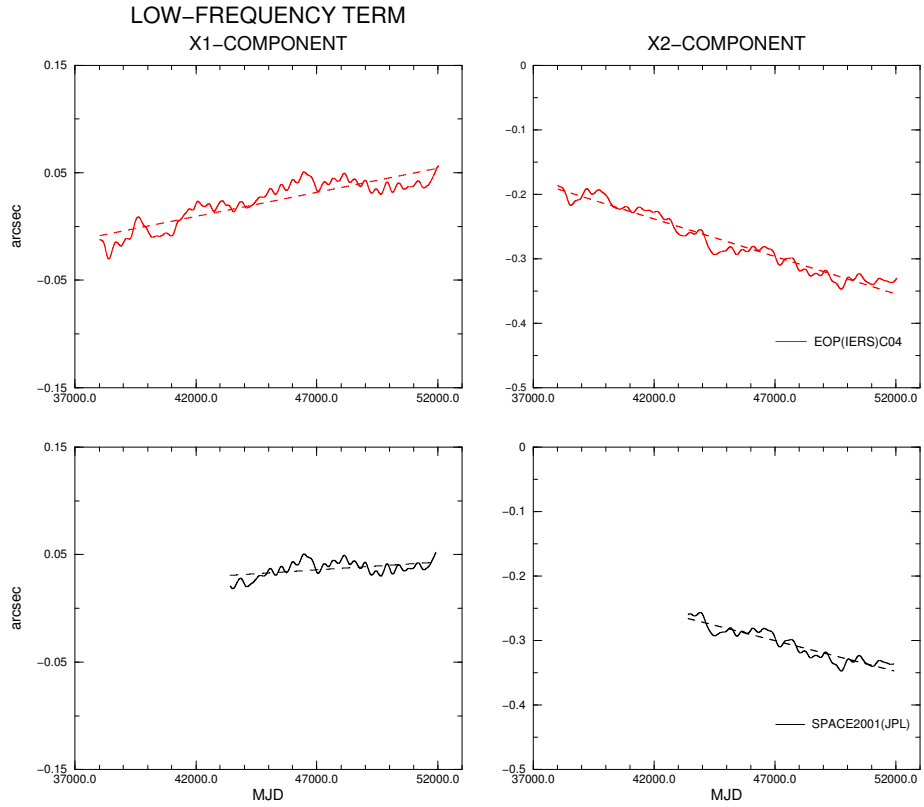

Figure 5. The low-frequency term of polar motion in the x_1-component (left side) and the x_2-component (right side). On each side, the motions shown are filtered out from the EOP(IERS)C04 (top), and SPACE2001(JPL) time series (bottom). Linear trends are indicated as dashed lines.

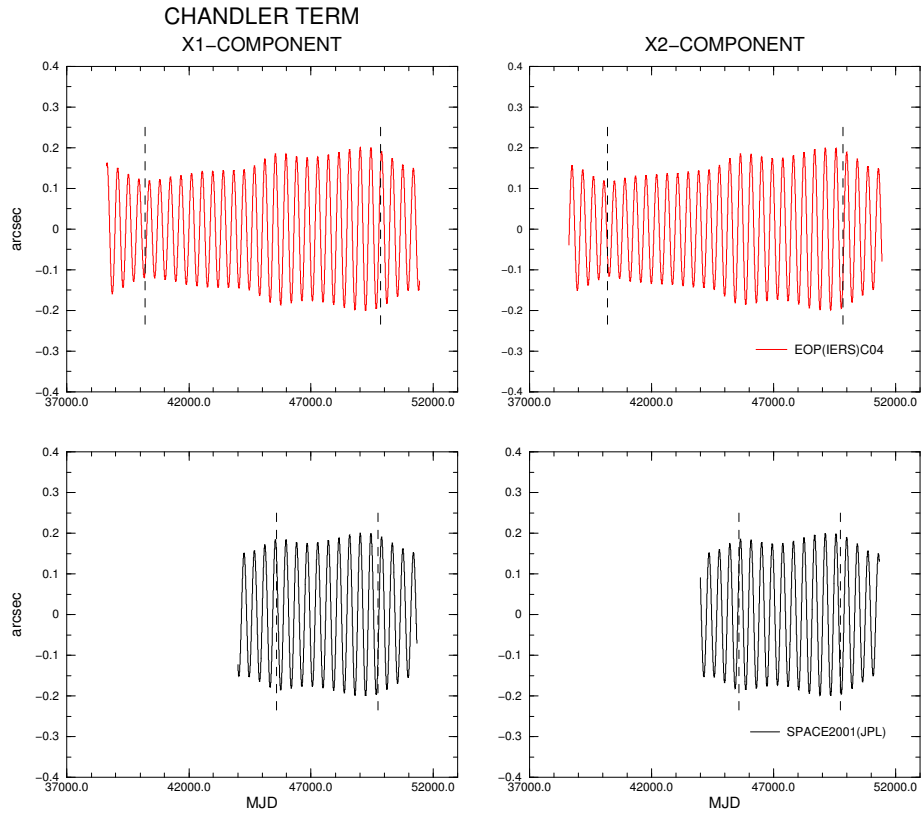

Figure 6. The Chandler term of polar motion in the x_1-component (left side) and the x_2-component (right side). On each side, the motions shown are filtered out from the EOP(IERS)C04 (top), and SPACE2001(JPL) time series (bottom). The time limits for the edge effects are indicated as dashed lines.

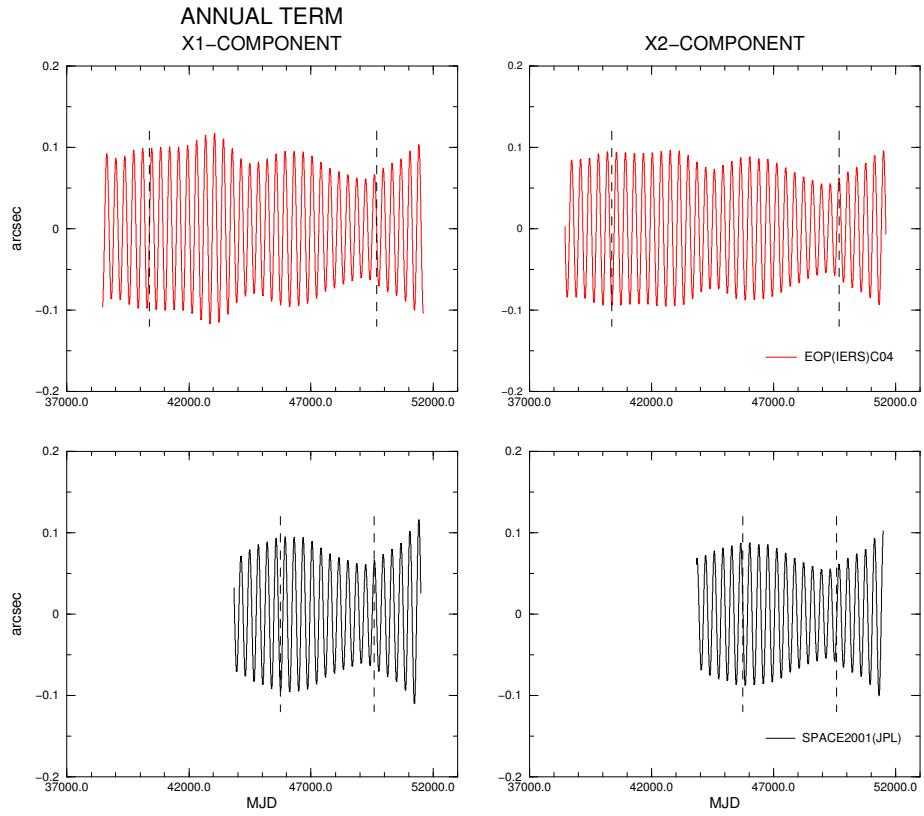

Figure 7. The annual term of polar motion in the x_1-component (left side) and the x_2-component (right side). On each side, the motions shown are filtered out from the EOP(IERS)C04 (top), and SPACE2001(JPL) time series (bottom). The time limits for the edge effects are indicated as dashed lines.

in Fig. 3 for the Chandler terms and in Fig. 4 for the annual terms. For the low-frequency, Chandler and annual terms filtered out from the EOP(IERS)C04 and SPACE2001(JPL) time series, see Figures 5 to 7. In these figures, the terms for the x_1-component are on the left-hand side and those for the x_2-component are on the right-hand side.

Using a simple unweighted least-squares fit to the filtered low-frequency terms for the x_1- and x_2-components, the linear trends of the rotation pole were estimated and are displayed as dashed lines in Figs. 2 and 5. Their results in terms of linear trend rates per year are summarized in Table 4. Note that the EOP(IERS)C01 estimates are based on the filtered low-frequency x_1- and x_2-data obtained from 1900.0 to 1999.0. Figure 8 shows for each PM time series the low-frequency part of polar motion and its linear trend in the plane of x_1 and x_2. To show the periodic signals contained within the low-frequency terms from the three longest PM time series, the prograde, retrograde and total amplitude spectra are computed by Fast Fourier Transform (FFT) and are presented in Fig. 9.

Concerning the edge effect of the recursive band-pass filtering, the fact exist that the number of estimates is effected at the beginning and the end of the resulting time series for the one term as used in each filtering for the other term and vice versa. Here, the estimates become gradually better over this time span at the beginning and worse over this time span at the end. For the number of estimates of the Chandler and annual terms at the different time sampling intervals, see Table 2. In the case of the Chandler terms, the time span for edge-effected estimates is ca. 4.3 years, and, in the case of the annual terms, ca. 5.2 years. Note that the time limits for the edge effects are indicated as dashed lines in Figs. 3, 4, 6 and 7. We found that this effect in the Chandler terms for the x_1- and x_2-components reaches 0.06 arcseconds from the EOP(IERS)C01 time series, but only 0.01 arcseconds from the SPACE2001(JPL) time series. For the annual terms, it reaches 0.08 arcseconds from EOP(IERS)C01 time series, but only 0.02 arcseconds from the SPACE2001(JPL) time series. Also, compare the EOP(IERS)C04 and SPACE2001(JPL) curves of the Chandler and annual wobbles given in the Appendix A, Figures A1 and A2, in particular at the beginning of the SPACE2001(JPL) curves, i.e. in both figures from picture (1).

In order to quantify and better describe the parameter variability of the periodic oscillations of polar motion over time, we need to use the polar coordinate system as reported in Höpfner (2002c+d, 2003). Therefore, we compute the radii, their direction angles and the period lengths for the Chandler and annual wobbles from the filtered PM terms in the Cartesian coordinate system. Moreover, we determine the semi-major axes a and semi-minor axes b as the maxima and minima of the radii and their directions γ_a and γ_b. Also, the numerical eccentricity ϵ used as a dimensionless measure for

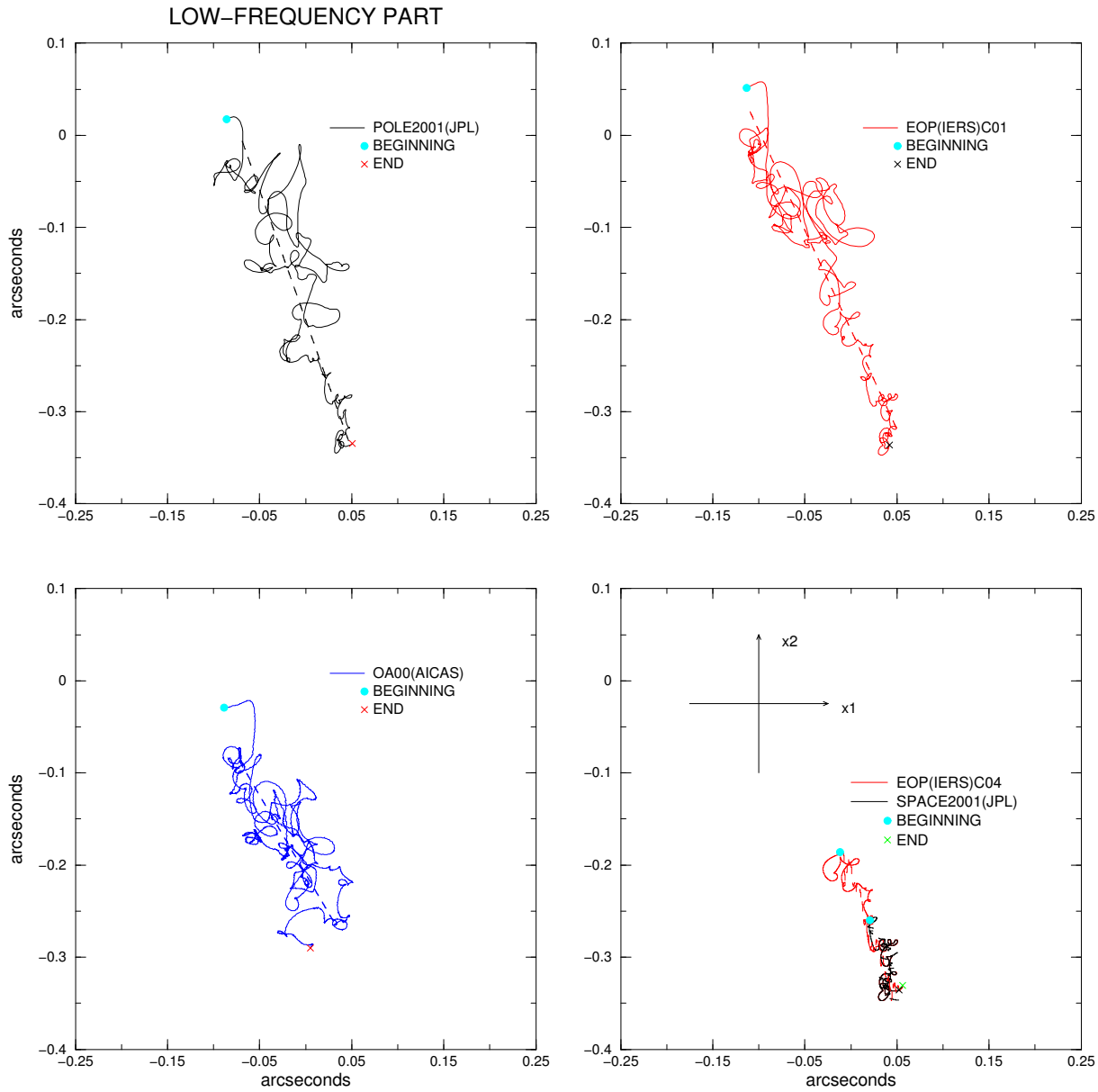

Figure 8. Low-frequency part of polar motion from the POLE2001(JPL)(top-left), EOP(IERS)C01 (top-right), OA00(AICAS) (bottom-left), EOP(IERS)C04 and SPACE2001(JPL) (both bottom-right) time series, each with its linear trend indicated as a dashed line. The x_1-axis points towards the Greenwich meridian, and the x_2-axis towards 90°East longitude. The beginning of each curve is indicated by a filled circle, and the end by a cross.

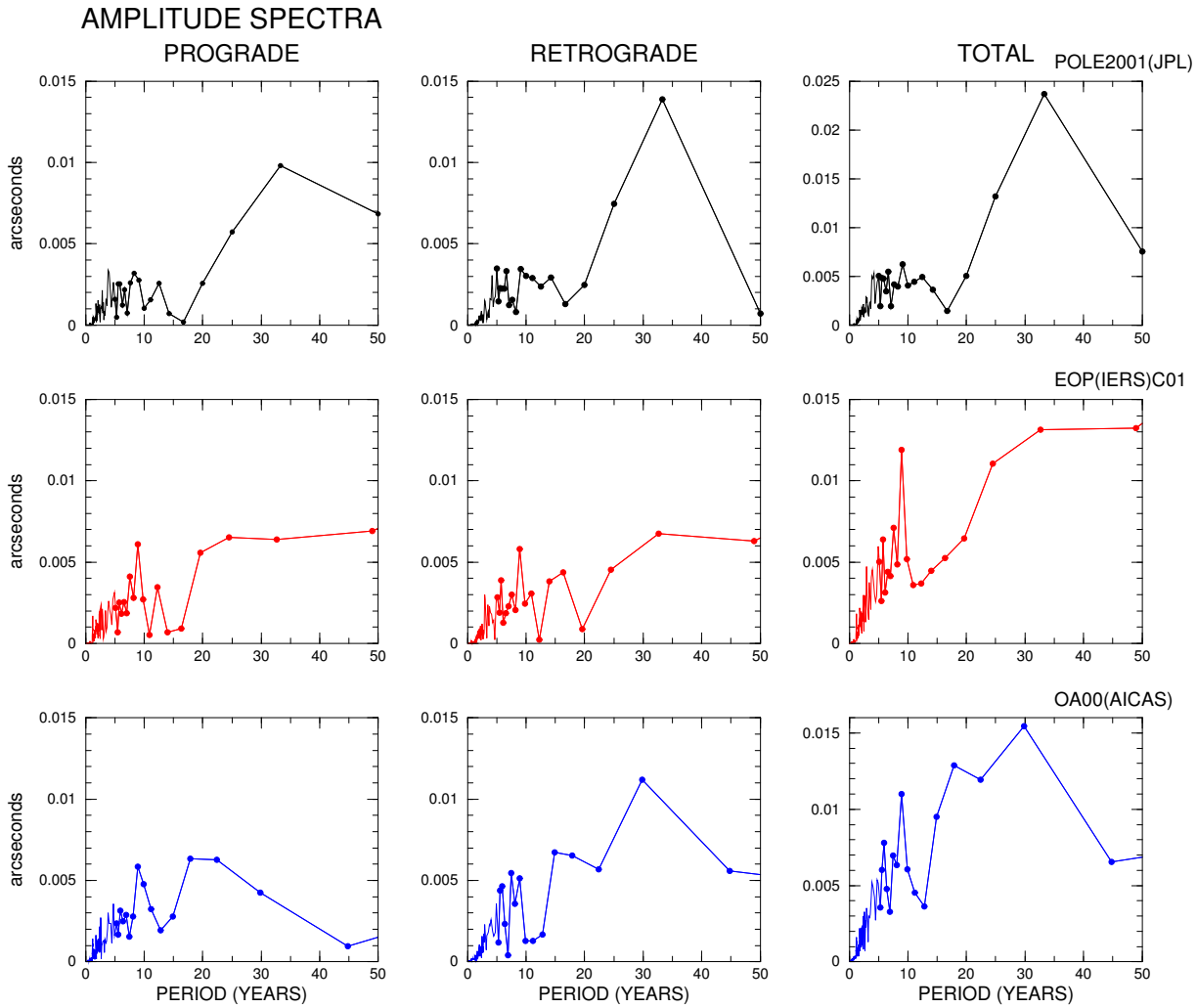

Figure 9. Amplitude spectra of low-frequency part of polar motion from the POLE2001(JPL) (top), EOP(IERS)C01 (centre), and OA00(AICAS) time series (bottom), with the prograde, retrograde and total spectra (from left to right).

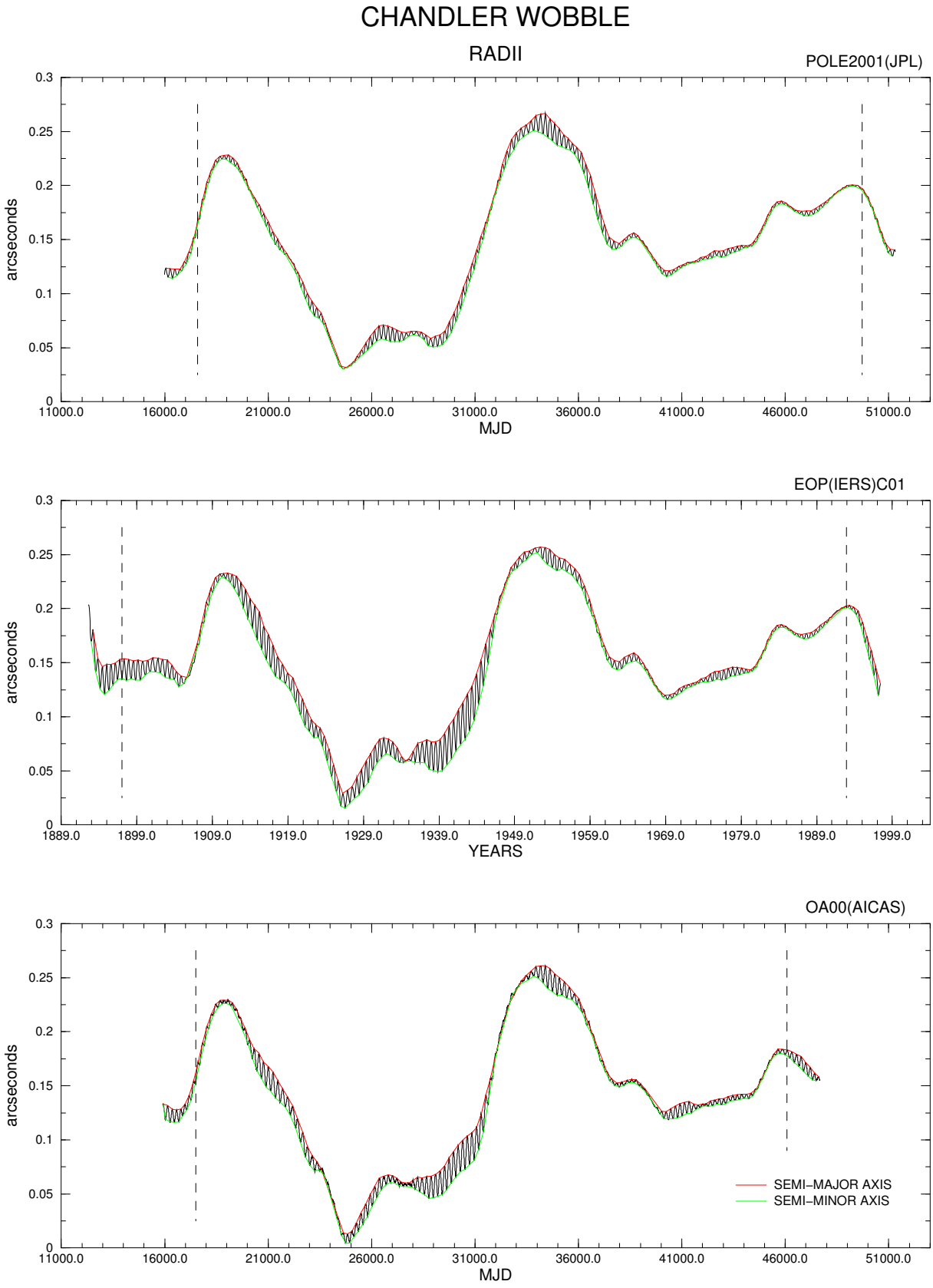

Figure 10. Variations in the radii of the Chandler wobble of polar motion from the POLE2001(JPL) (top), EOP(IERS)C01 (centre), and OA00(AICAS) time series (bottom). In each panel, the curves shown are: Radii (in black), semi-major axes (in red) and semi-minor axes (in green). The time limits for the edge effects are indicated as dashed lines.

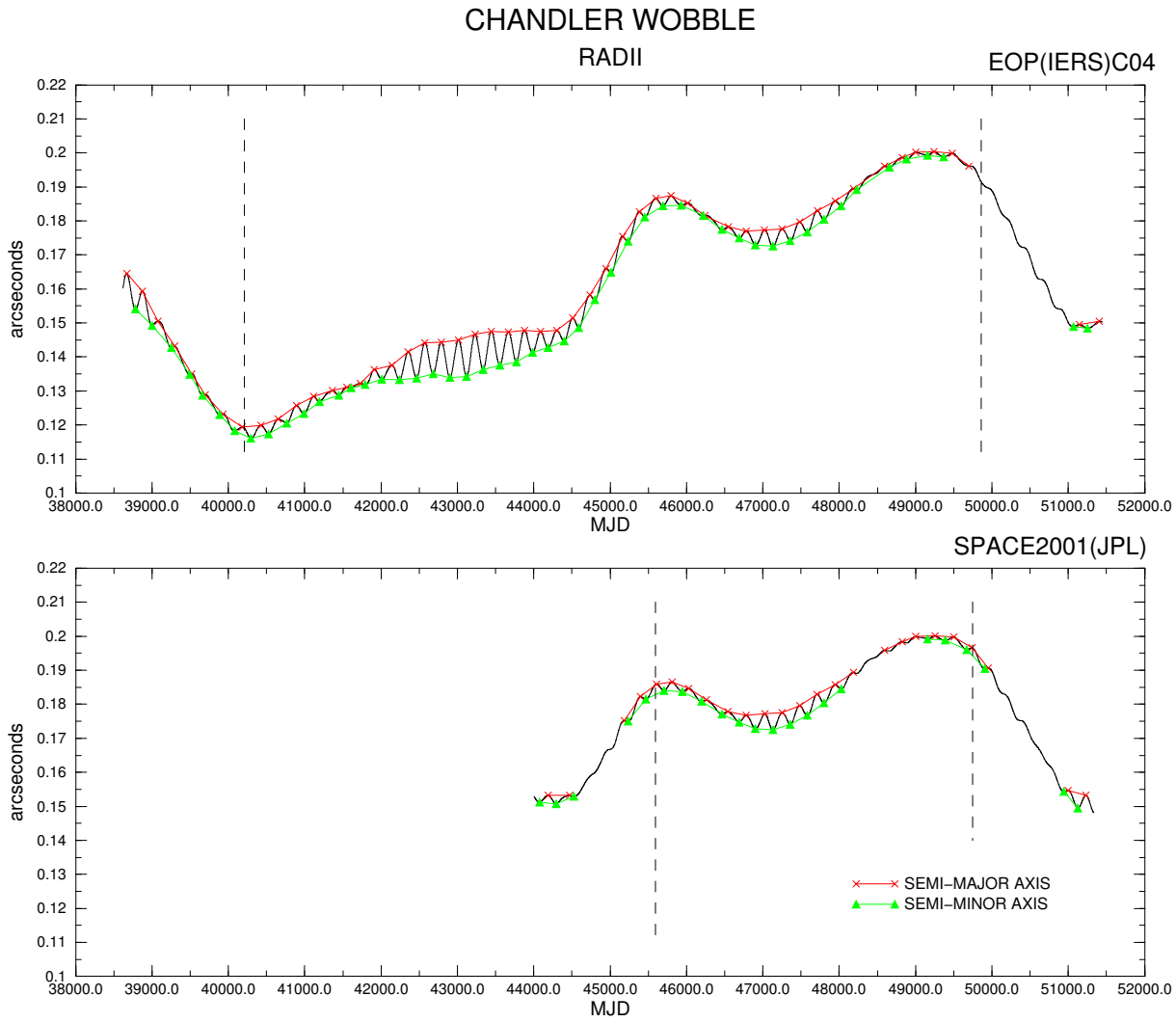

Figure 11. Variations in the radii of the Chandler wobble of polar motion from the EOP(IERS)C04 (top), and SPACE2001(JPL) time series (bottom). In each panel, the curves shown are: Radii (in black), semi-major axes (in red) and semi-minor axes (in green). The time limits for the edge effects are indicated as dashed lines.

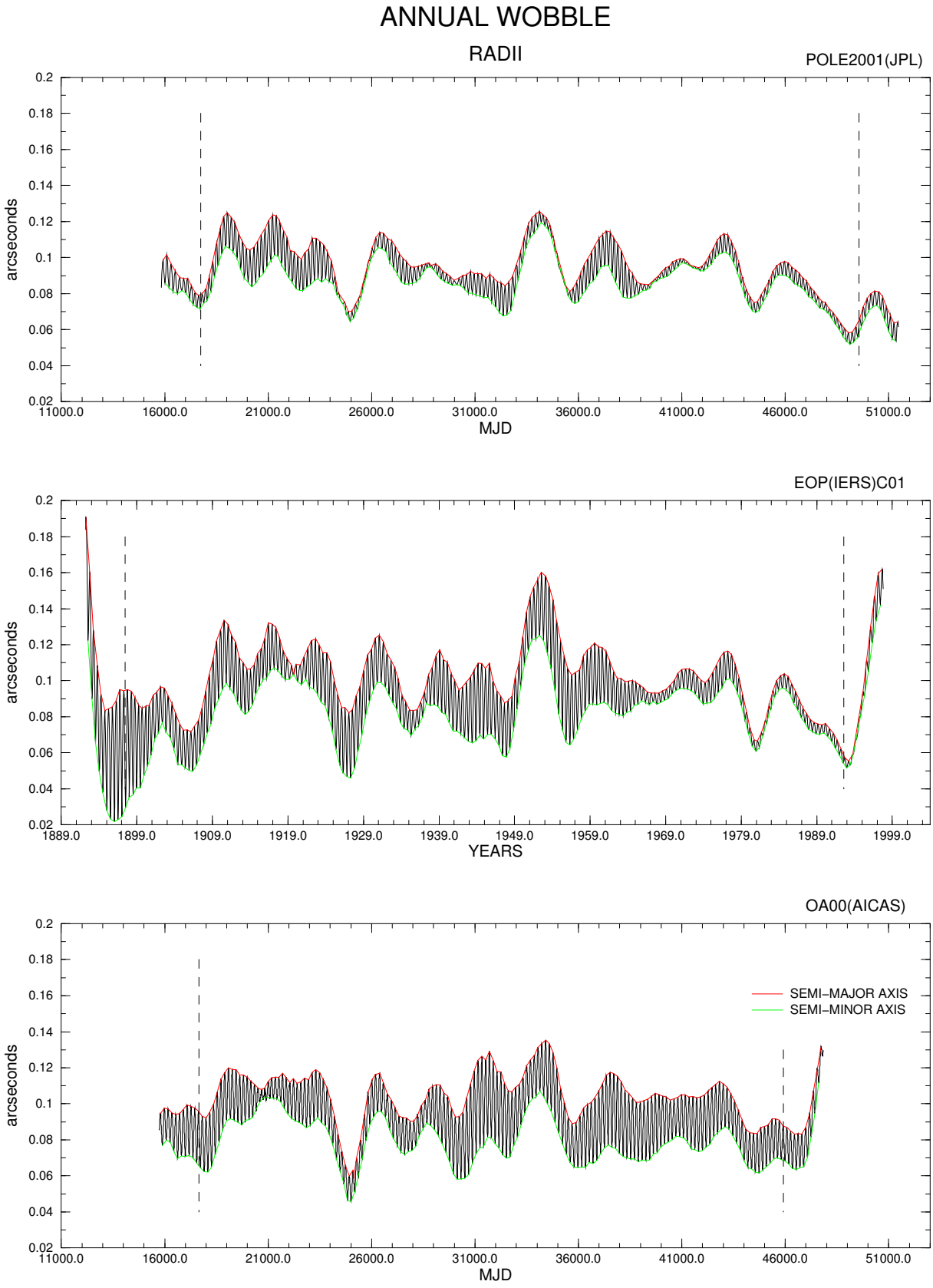

Figure 12. Variations in the radii of the annual wobble of polar motion from the POLE2001(JPL) (top), EOP(IERS)C01 (centre), and OA00(AICAS) time series (bottom). In each panel, the curves shown are: Radii (in black), semi-major axes (in red) and semi-minor axes (in green). The time limits for the edge effects are indicated as dashed lines.

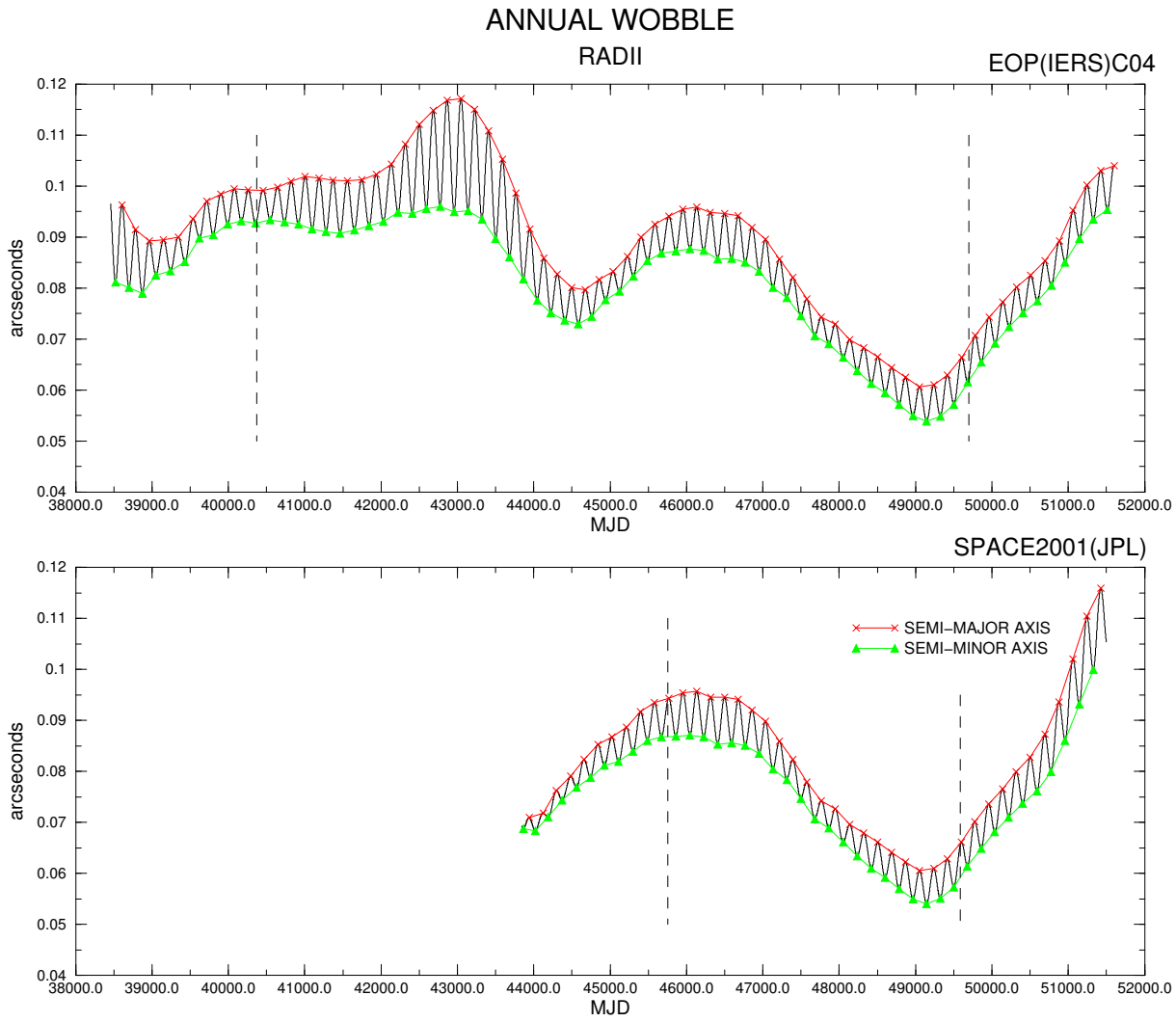

Figure 13. Variations in the radii of the annual wobble of polar motion from the EOP(IERS)C04 (top), and SPACE2001(JPL) time series (bottom). In each panel, the curves shown are: Radii (in black), semi-major axes (in red) and semi-minor axes (in green). The time limits for the edge effects are indicated as dashed lines.

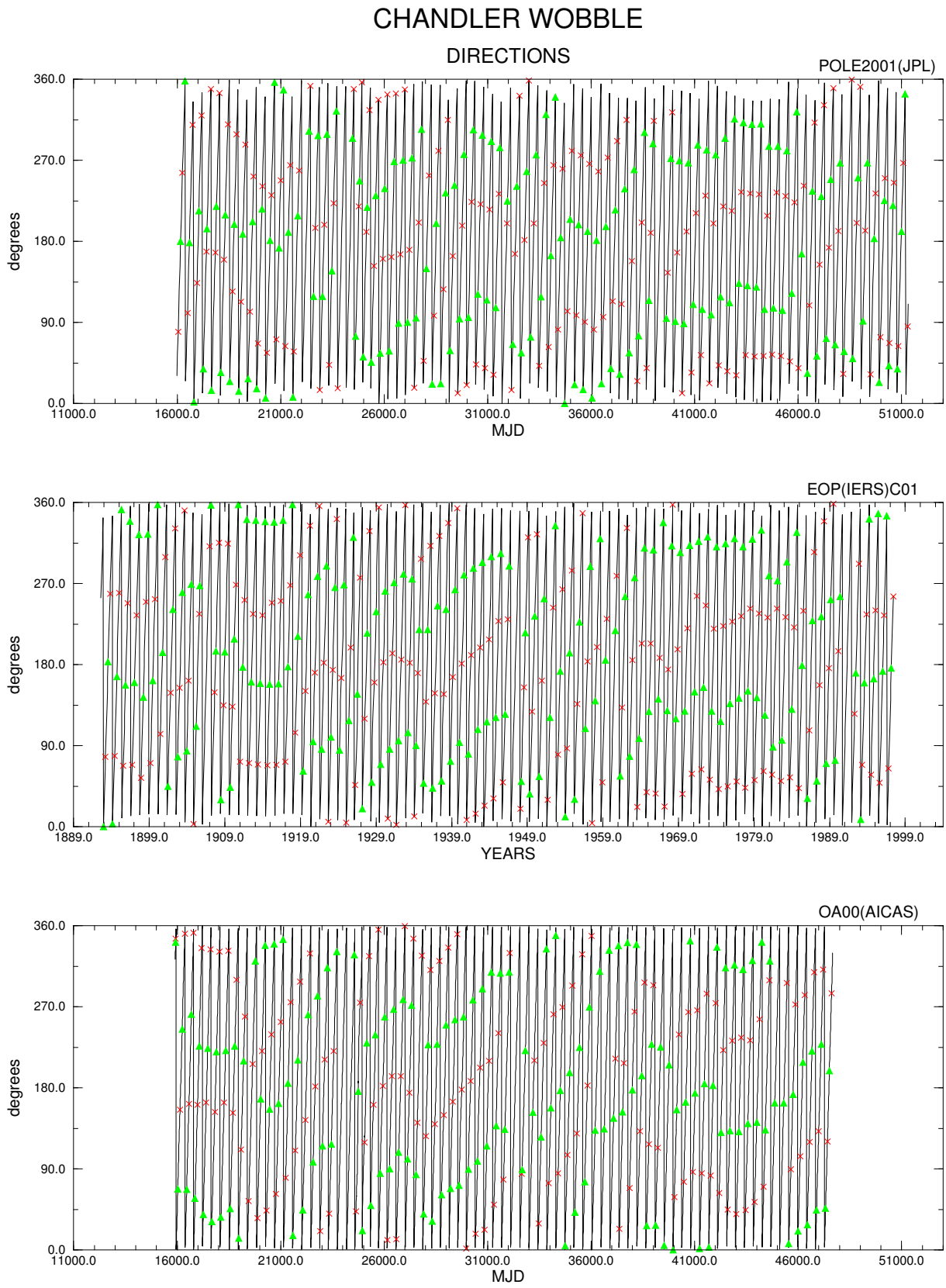

Figure 14. The direction courses of the radii of the Chandler wobble of polar motion from the POLE2001(JPL) (top), EOP(IERS)C01 (centre), and OA00(AICAS) time series (bottom). In each panel, the markers used are crosses (in red) indicating the direction angles of the maximum radii (semi-major axes) and triangles (in green) indicating the direction angles of the minimum radii (semi-minor axes).

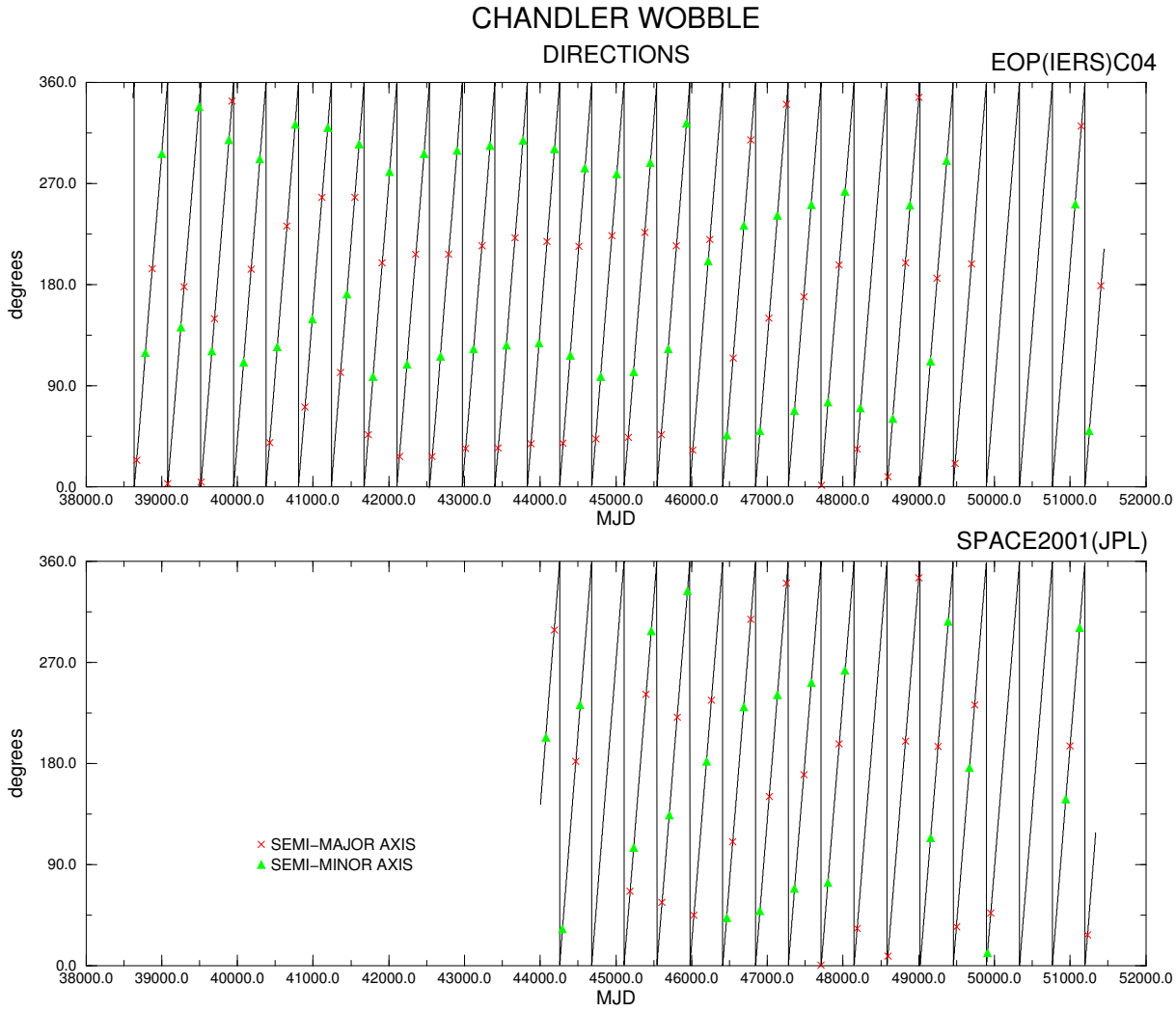

Figure 15. The direction courses of the radii of the Chandler wobble of polar motion from the EOP(IERS)C04 (top) and SPACE2001(JPL) time series (bottom). In each panel, the markers used are crosses (in red) indicating the direction angles of the maximum radii (semi-major axes) and triangles (in green) indicating the direction angles of the minimum radii (semi-minor axes).

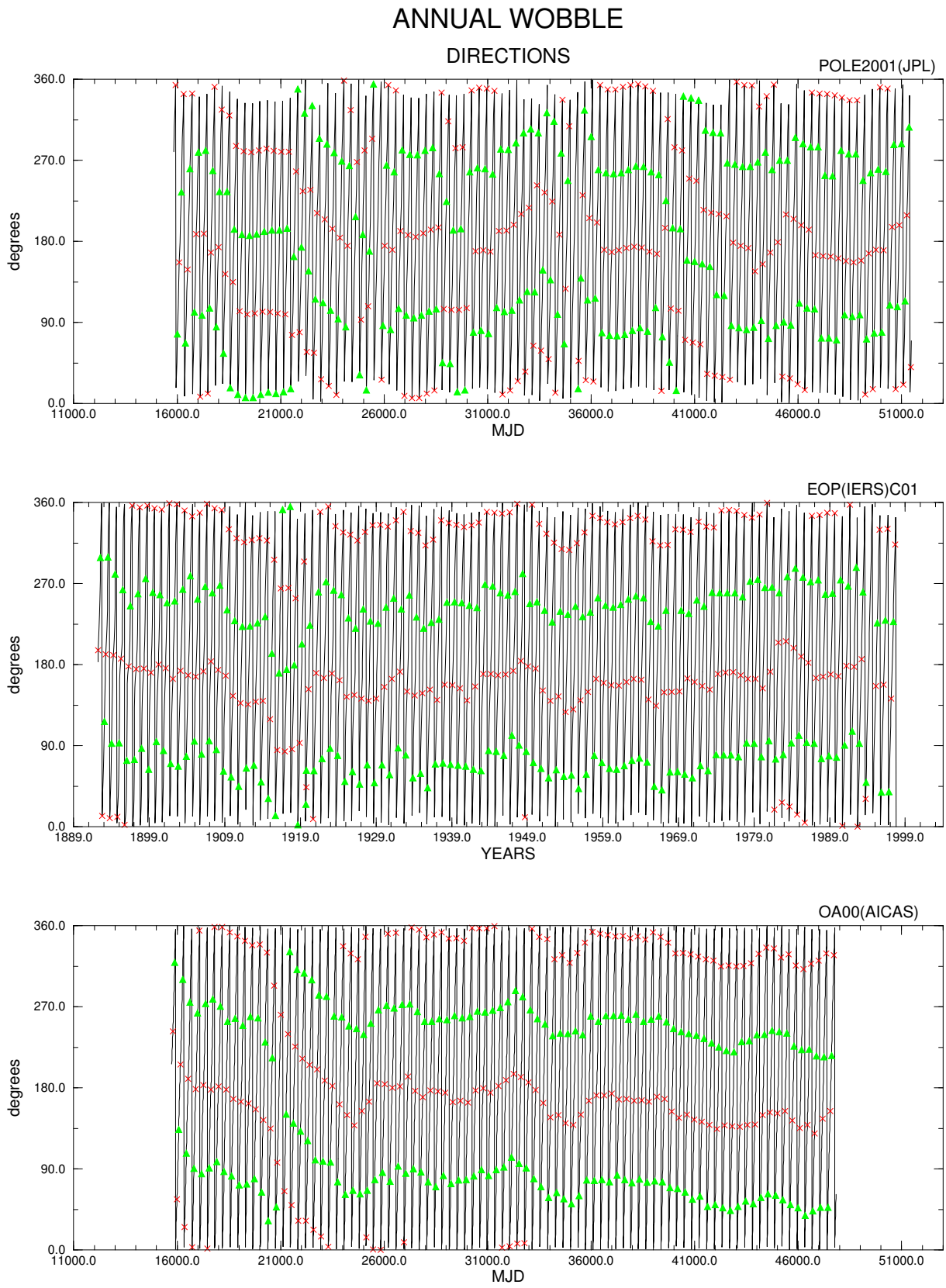

Figure 16. The direction courses of the radii of the annual wobble of polar motion from the POLE2001(JPL) (top), EOP(IERS)C01 (centre), and OA00(AICAS) time series (bottom). In each panel, the markers used are crosses (in red) indicating the direction angles of the maximum radii (semi-major axes) and triangles (in green) indicating the direction angles of the minimum radii (semi-minor axes).

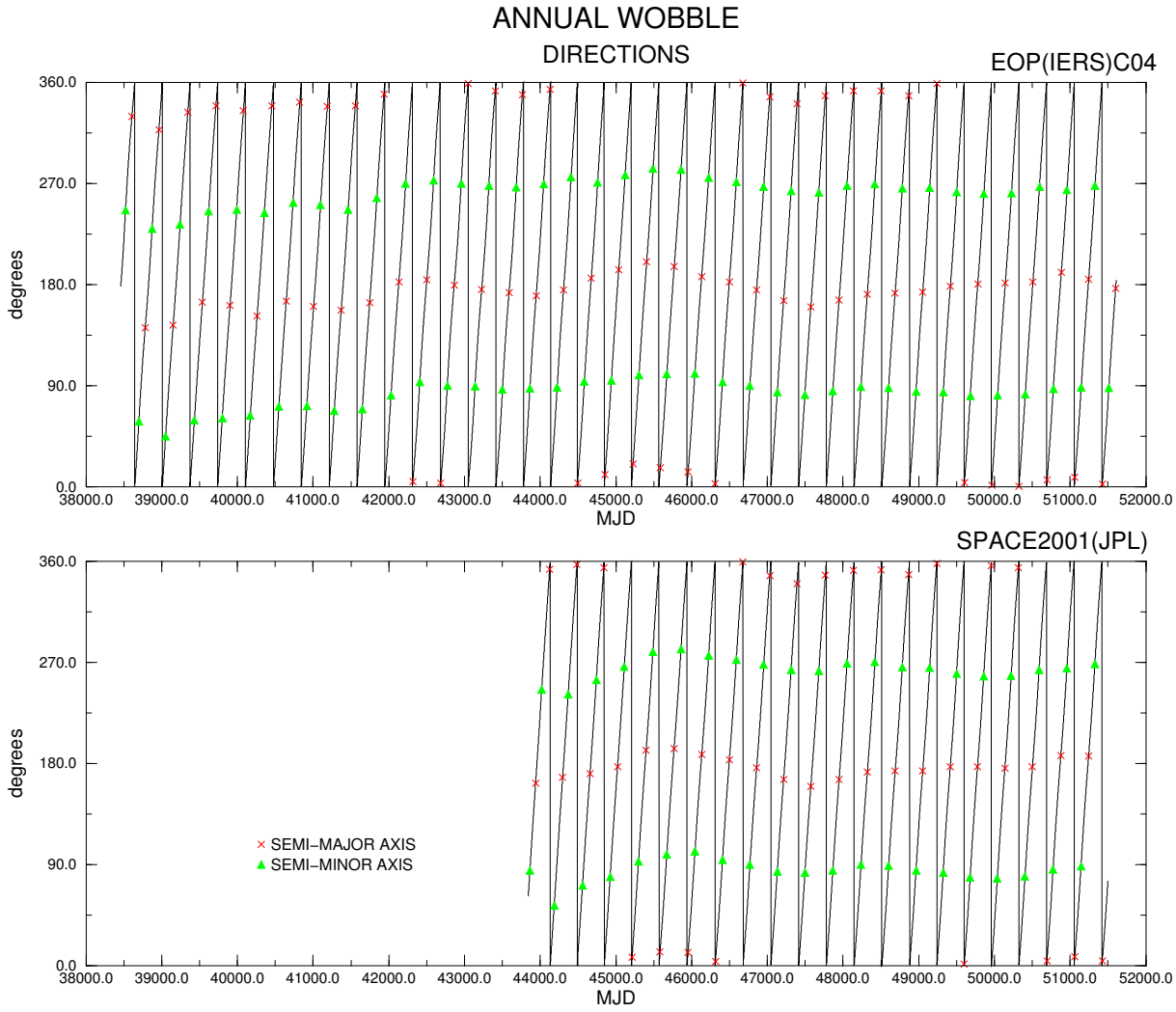

Figure 17. The direction courses of the radii of the annual wobble of polar motion from the EOP(IERS)C04 (top) and SPACE2001(JPL) time series (bottom). In each panel, the markers used are crosses (in red) indicating the direction angles of the maximum radii (semi-major axes) and triangles (in green) indicating the direction angles of the minimum radii (semi-minor axes).

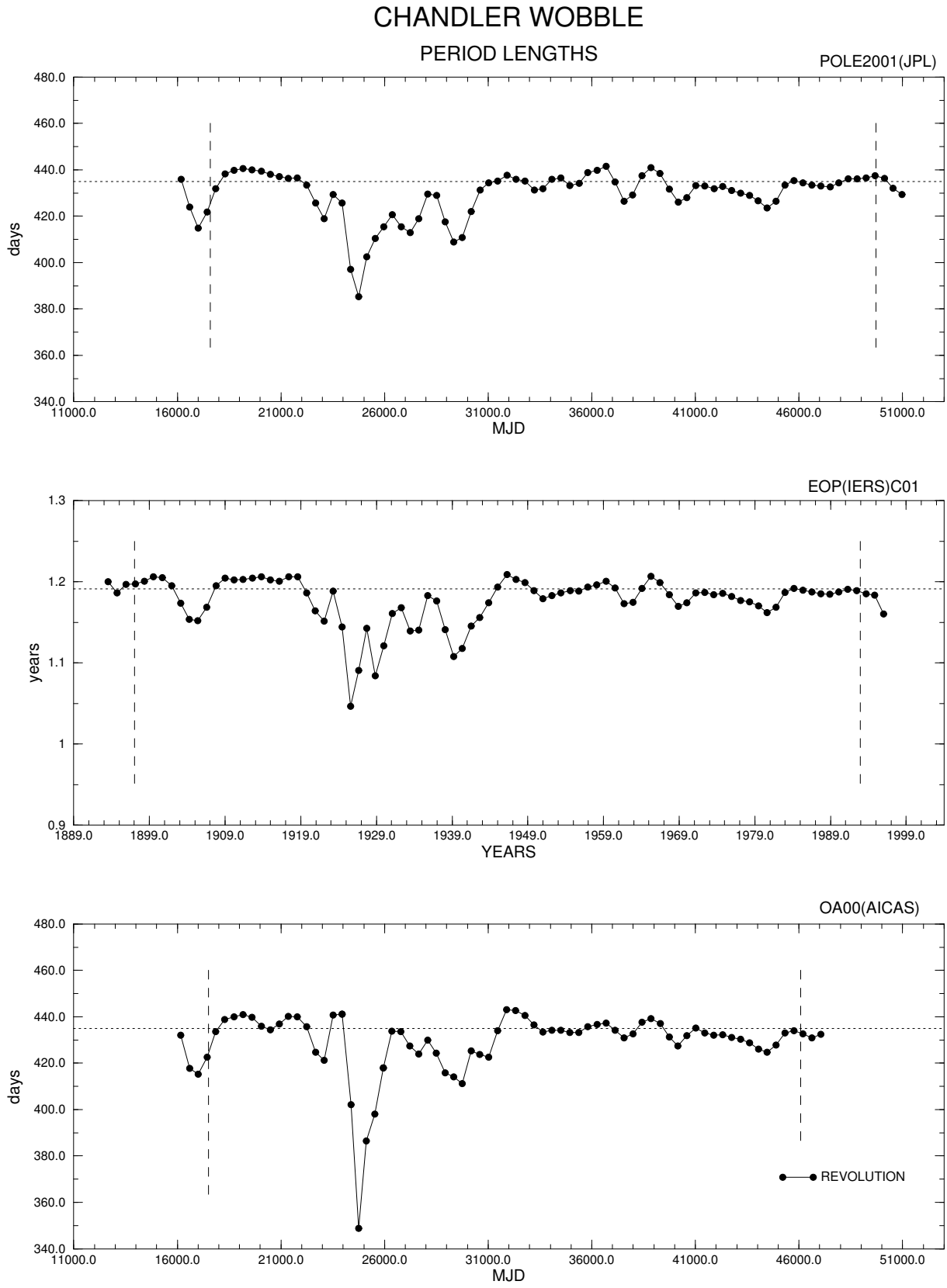

Figure 18. Variation in the period of the Chandler wobble of polar motion from the POLE2001(JPL) (top), EOP(IERS)C01 (centre), and OA00(AICAS) time series (bottom). In each panel, the dotted line indicates the 435-day (or 1.191-year) baseline. The time limits for the edge effects are indicated as dashed lines.

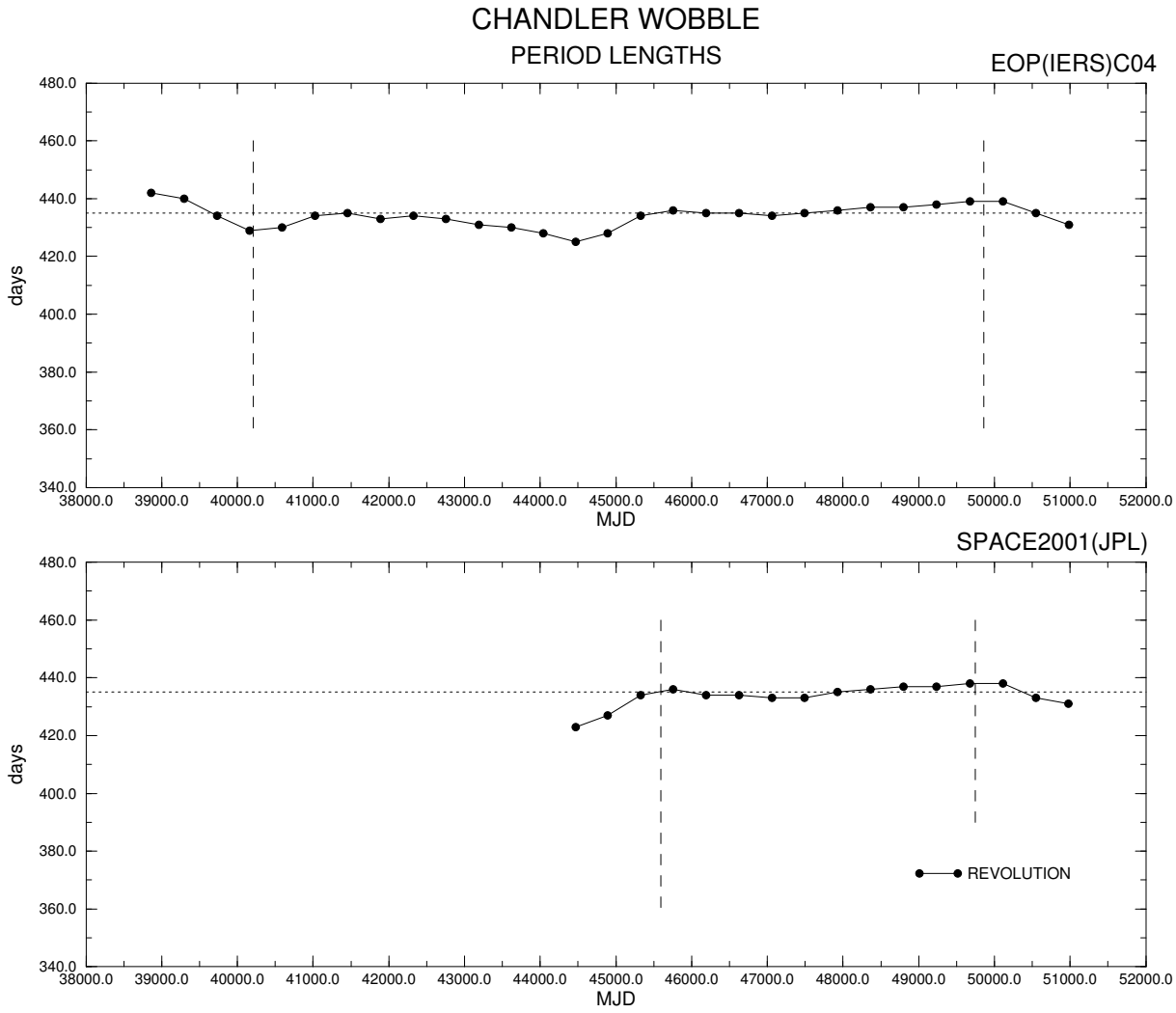

Figure 19. Variation in the period of the Chandler wobble of polar motion from the EOP(IERS)C04 (top), and SPACE2001(JPL) time series (bottom). In each panel, the dotted line indicates the 435-day baseline. The time limits for the edge effects are indicated as dashed lines.

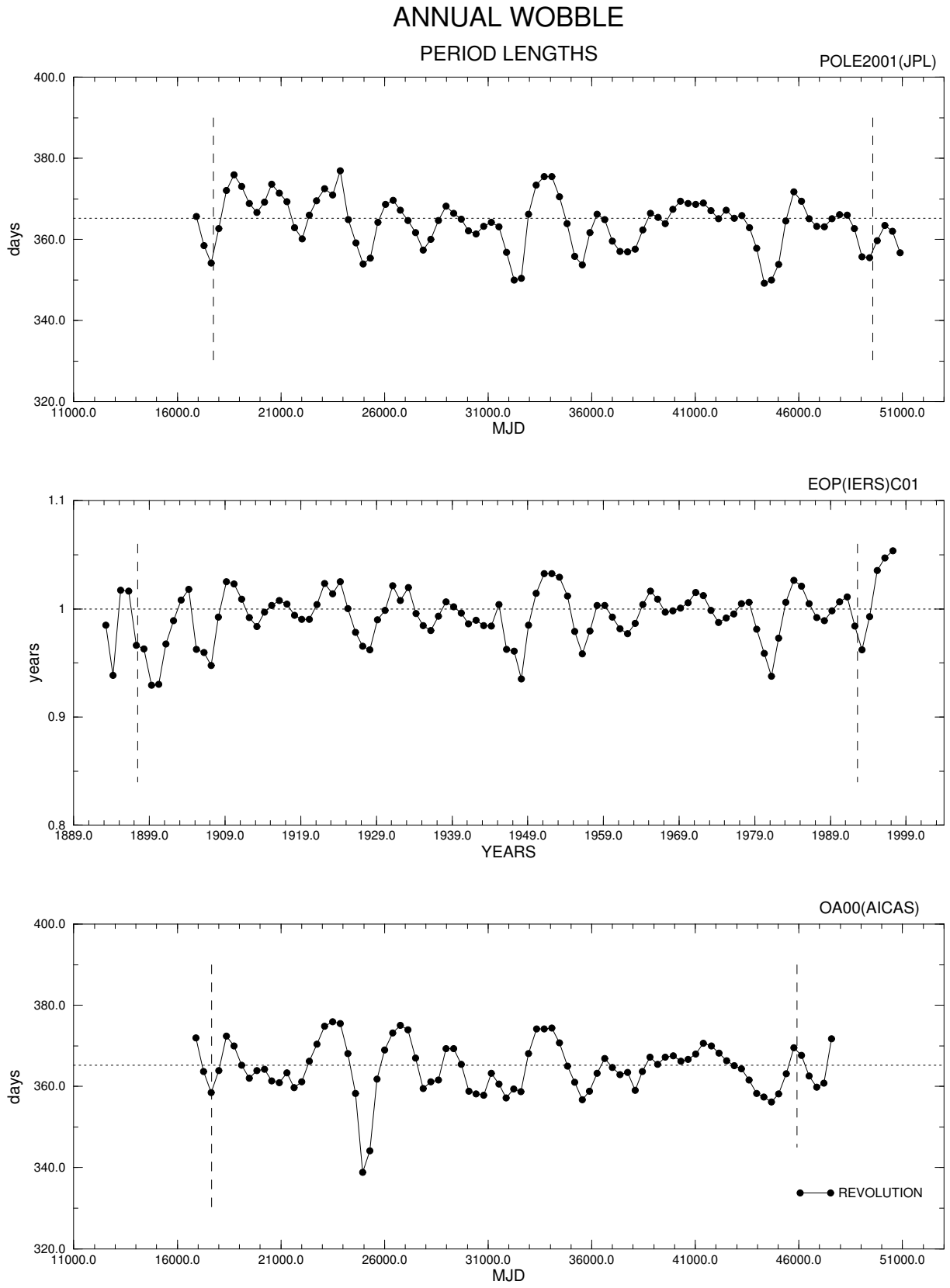

Figure 20. Variation in the period of the annual wobble of polar motion from the POLE2001(JPL) (top), EOP(IERS)C01 (centre), and OA00(AICAS) time series (bottom). In each panel, the dotted line indicate the 365-day (or 1-year) baseline. The time limits for the edge effects are indicated as dashed lines.

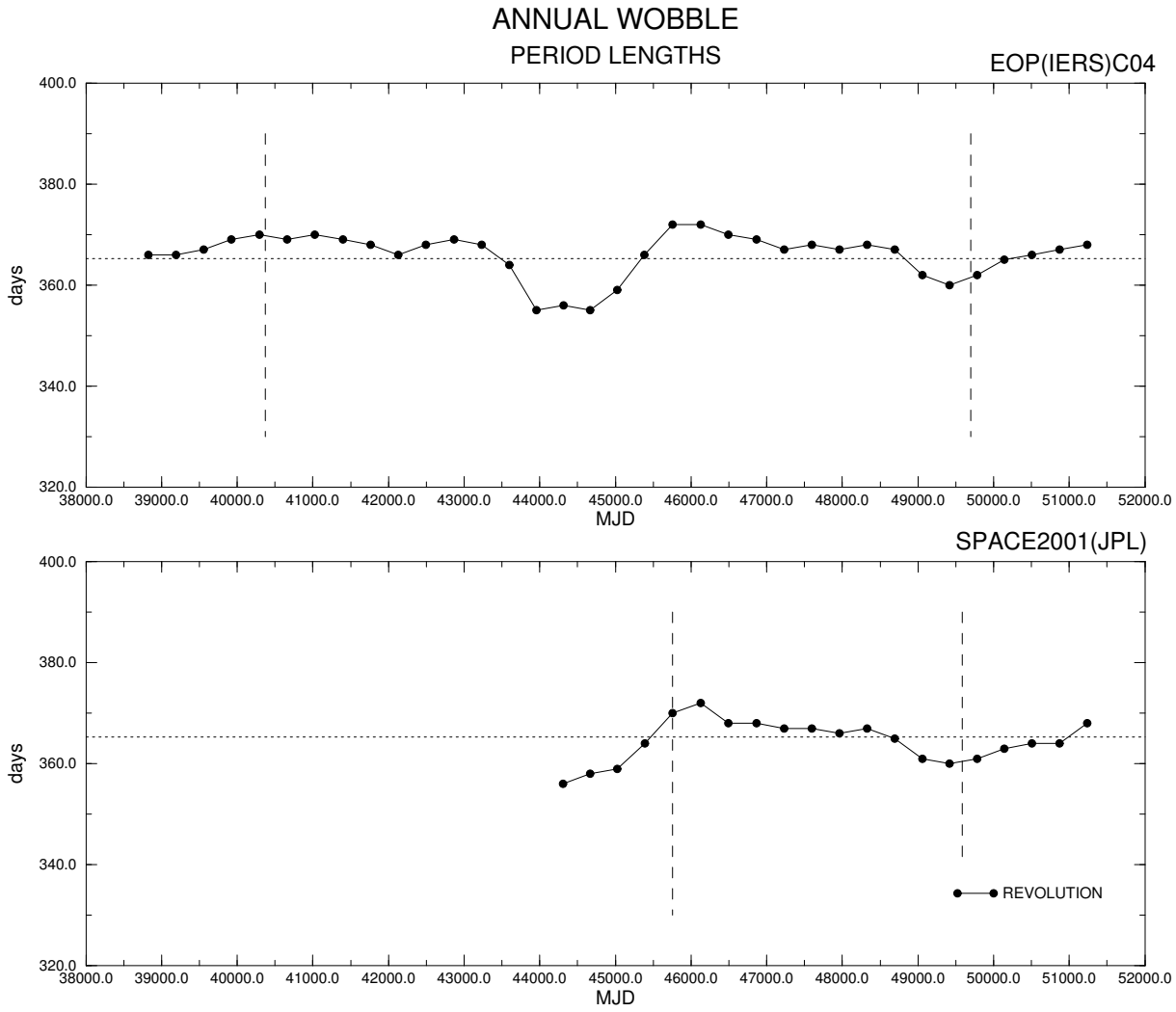

Figure 21. Variation in the period of the annual wobble of polar motion from the EOP(IERS)C04 (top), and SPACE2001(JPL) time series (bottom). In each panel, the dotted line indicates the 365-day baseline. The time limits for the edge effects are indicated as dashed lines.

the ellipticity of a periodic motion is calculated. A summary of the formulae used here is given in Höpfner (2002c+d).

To assess the parameter estimates of a periodic motion derived in the polar coordinate system, the following characteristics need to be noted:
- The smaller the difference between the semi-major and semi-minor axes, the more circular is the periodic component of polar motion, while the larger the difference, the more elliptic is the periodic component.
- If the direction angle increases, then the motion is prograde, i.e. counter-clockwise; if it decreases, then the motion is retrograde, i.e. clockwise.
- Each direction course of 0^o to 360^o (or vice versa of 360^o to 0^o) indicates an elapsed prograde (retrograde) revolution of the PM component of interest, with its turning-points indicating the extreme sites (maxima and minima of the radii) of the component.
- The more straight the direction course over a revolution, the more circular is the periodic motion. Conversely, the more curved the direction course, the more elliptic is the motion.
- An elliptic motion cycle should exhibit two maximum and two minimum radii. However, if a cycle elapsed as a quasi-circular spiral, any number of them could be missing.
-If $\epsilon = 0$, then there is a circular motion; if $0 < \epsilon < 1$, then there is an elliptic motion. The closer ϵ is to 0, the more circular is its motion; while the closer ϵ is to 1, the more elliptic is its motion.
- The shorter the time sampling interval of a time series, the better defined are the maxima as sites for the semi-major axes and the minima as sites for the semi-minor axes, for both magnitude and direction. Table 5 presents for the Chandler and annual wobbles the mean direction change of the radius at the different sampling intervals of the PM time series.

Table 5. Time sampling interval and mean direction change of Chandler and annual wobbles radii

PM time series	Sampling interval	Direction change of the radius for the Chandler wobble	Direction change of the radius for the annual wobble
POLE2001(JPL)	30.4375 days	25.8^o	30.0^o
EOP(IERS)C01	0.05 years	15.5^o	18.0^o
OA00(AICAS)	5.034652 days	4.26^o	4.96^o
EOP(IERS)C04	1 day	0.85^o	0.99^o
SPACE2001(JPL)	1 day	0.85^o	0.99^o

For the Chandler wobble of polar motion, variations in the radii from the POLE2001(JPL), EOP(IERS) C01, and OA00(AICAS) time series over time are presented in Fig. 10 and those from the EOP(IERS)C04 and SPACE2001(JPL) time series in Fig. 11. The same for the annual wobble are shown in Figs. 12 and 13. Note how with the radius variation, the superior envelope indicates the change in the semi-major axis and the inferior envelope indicates the change in the semi-minor axis. The direction courses of the radii are displayed in Figs. 14 to 17, with markers indicating the direction angles of the semi-major and semi-minor axes, and the period variations in Figs. 18 to 21, with the dashed line indicating a baseline of 435 days (or 1.191 years) for the Chandler wobble and of 365 days (or 1 year) for the annual wobble. Figures 14 and 15 present the direction courses of the radii of the Chandler wobble of polar motion, and Figs. 16 and 17 those of the annual wobble. Figures 18 and 19 show the variations in the Chandler period, and Figs. 20 and 21 the variations in the annual period.

Table 6. Relevant characteristics of the Chandler and annual wobbles

Wobble	Period (days)	Motion direction	Type	Numerical eccentricity	Semi-major axis (arcsec)	Direction of the semi-major axis	Semi-minor axis (arcsec)
Chandler	410 ... 442	prograde	quasi-circular	0.00 ... 0.70	0.03 ... 0.27	very variable	0.02 ... 0.25
Annual	356 ... 376	prograde	elliptic	0.20 ... 0.80	0.05 ... 0.16	138^o ... 195^o	0.04 ... 0.13

The relevant characteristics of the Chandler and annual wobbles, in particular the period length, motion direction, type of motion, numerical eccentricity, semi-major axis and its direction angle and semi-minor axis, are summarized in Table 6. Figure 22 shows selected cycles of the Chandler (upper part) and annual wobbles (lower part). For each example, the same motion cycle is derived from the POLE2001(JPL), EOP(IERS)C01, OA00(AICAS), EOP(IERS)C04, and SPACE2001(JPL) time series, where the POLE2001(JPL) and EOP(IERS)C01 cycles are plotted with their sampling points in panels (a) and (b). Note that the Chandler cycle that elapsed from MJD 45108.0 to 45541.0, i.e. from May 1982 to July 1983, has the number (4) and the annual cycle that elapsed from MJD 45940.0 to 46310.0, i.e. from August 1984 to September 1985, the number (7) in our other figures (e.g., in the Appendix A).

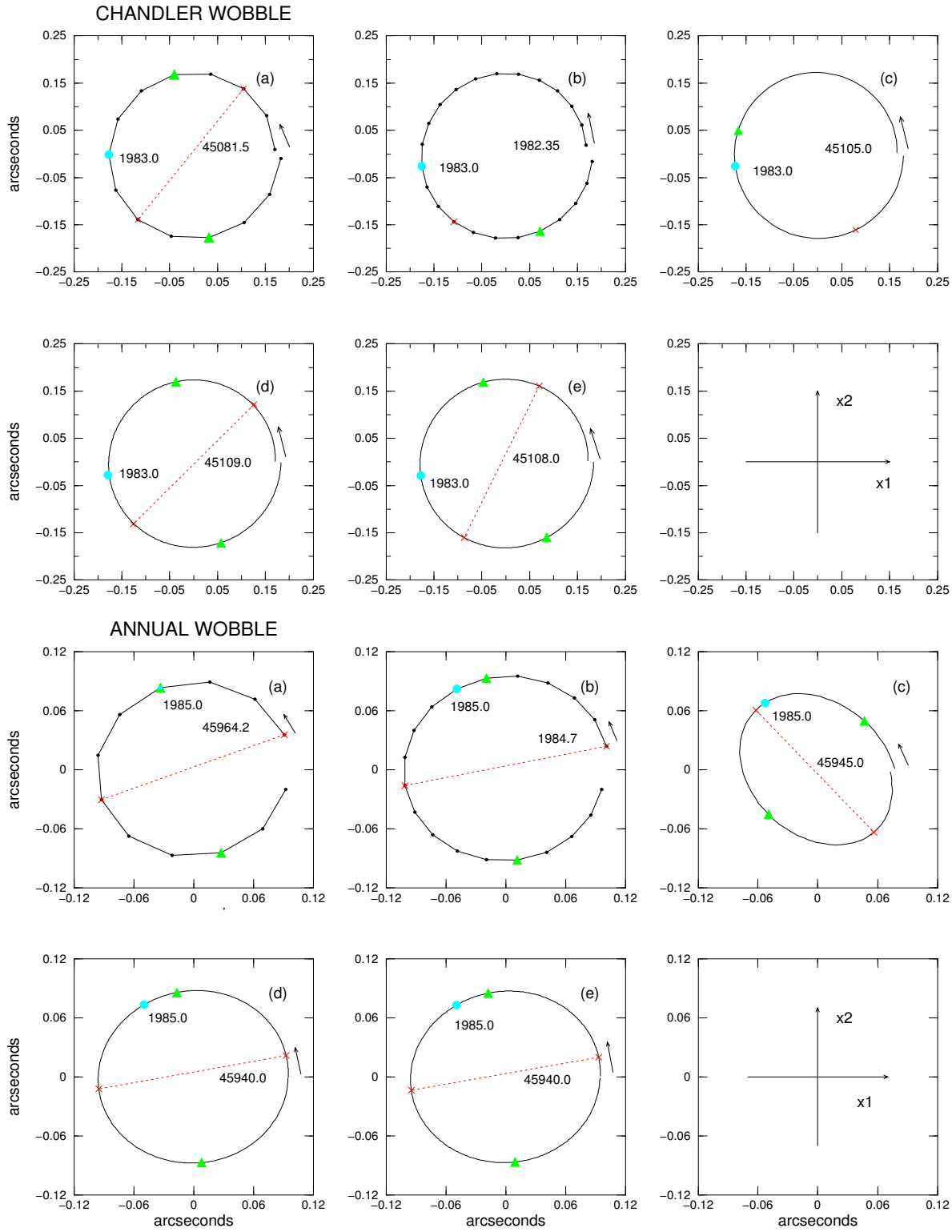

Figure 22. A cycle of the Chandler wobble (upper part) and of the annual wobble (lower part). In each part, the curves shown are the same motion cycle from the POLE2001(JPL) (a), EOP(IERS)C01 (b), OA00(AICAS) (c), EOP(IERS)C04 (d), and SPACE2001(JPL) time series (e). The x_1-axis points towards the Greenwich meridian, and the x_2-axis towards 90°East longitude. The markers used are crosses in red at the maxima and triangles in green at the minima. Also indicated is the beginning of a year by a filled circle in cyan.

Relative to the EOP(IERS)C04 and SPACE2001(JPL) systems, the motion cycles of the Chandler and annual wobbles over the total analysis intervals are presented in the Appendix A, Figures A1 and A2, to illustrate the variability in radius (magnitude), ellipticity and the orientation of elliptic motion. More details about the parameter variability of the Chandler and annual wobbles derived from the SPACE99(JPL) time series can be found in Höpfner (2002a+d). For a comparison of PM estimates, especially for the Chandler and annual wobbles at the Potsdam Observatory, see the Appendix B, Figures B1 and B2. Also note that estimates for the semi-Chandler and semi-annual wobbles are included in these figures.

4 Discussion of the results

As part of the discussion, we will use other recent studies in this field as published by Nastula et al. (1993), Vicente and Wilson (1997, 2002), Vondrák (1999), Gross and Vondrák (1999), Liu et al. (2000), and Schuh et al. (2000, 2001); see Section 1. Concerning our solutions, it should be noted that they have the same time sampling intervals as their input PM time series employed; see Section 2.

Low-frequency part of polar motion (Tables 4 and 7, Figures 2, 5, 8 and 9)

As seen in Figs. 2, 5 and 8, the secular polar motion is evident and re-confirmed. Comparing the curves of the low-frequency terms in the x_1-component and the x_2-component (plotted in Figs. 2 and 5), we find that there are similar variations with time. Also, their linear trends as obtained from the POLE2001(JPL), EOP(IERS)C01, and OA00(AICAS) time series over the long time spans are in good agreement, except the OA00(AICAS) trend in the x_2-component. Examing their 2-D motions in Fig. 8, it is noticed that the direction of the linear drift in the pole path is better fixed for POLE2001(JPL)and EOP(IERS)C01, including the recent PM data based on space-geodetic techniques.

Table 7. Recent estimates of the linear rate of the motion of the rotation pole

PM time series	Time span	Linear trend rate		Source
		Magnitude	Direction	
		mas/year	° West	
POLE99(JPL)	1900 ... 1999	3.54	69.92	Vicente and Wilson (2002)
POLE2001(JPL)	1900 ... 2001	3.530 ± 0.019	70.46 ± 0.32	This study
EOP(IERS)C01	1900 ... 1992	4.43 ± 0.08	78.15 ± 1.00	Schuh et al. (2000, 2001)
EOP(IERS)C01	1900 ... 1999	3.35	76.3	Vicente and Wilson (2002)
EOP(IERS)C01	1900 ... 2000	3.901 ± 0.022	65.17 ± 0.22	This study
OA (AICAS)	1900 ... 1992	3.51 ± 0.01	79.2 ± 0.2	Gross and Vondrák (1999)
OA (AICAS)	1900 ... 1992	3.20	77.1	Vondrák (1999)
OA97(AICAS)	1900 ... 1992	3.31 ± 0.05	76.1 ± 0.8	Schuh et al. (2000, 2001)
OA (AICAS)	1900 ... 1992	2.84	73.03	Vicente and Wilson (2002)
OA (AICAS)	1900 ... 1992	2.86	75.4	Vondrák (2000)
OA99(AICAS)	1900 ... 1992	2.81 ± 0.04	75.4 ± 0.9	Schuh et al. (2000, 2001)
OA00(AICAS)	1900 ... 1992	2.250 ± 0.010	59.58 ± 0.24	This study
EOP(IERS)C04	1962 ... 2002	4.554 ± 0.008	68.93 ± 0.09	This study
SPACE96(JPL)	1977 ... 1997	4.123 ± 0.002	73.9 ± 0.3	Gross and Vondrák (1999)
SPACE2001(JPL)	1977 ... 2002	3.521 ± 0.014	81.42 ± 0.17	This study

For comparison, our and other recent estimates of the linear trend rate of the rotation pole are listed in Table 7. Generally, we can say that the solutions are of similar magnitude and direction, except our OA00(AICAS) solution and those for EOP(IERS)C04, SPACE96(JPL) and SPACE2001(JPL) which cover relatively short time spans. The improved reanalyses of the latitude and universal time observations based on optical astrometry (Vondrák 2000) are especially noted for OA (AICAS). Therefore, for different versions, the estimates differ visibly in magnitude.

The PM time series studied here are to assess the preferred estimate of the linear trend rate. EOP(IERS) C01 is a Earth orientation series combined with the new EOP solution from optical astrometry observations and the IERS solution based on space-geodetic techniques having the greatest time span. Thus, the most reliable trend estimate is likely to be obtained from that time series. Accordingly, the Earth's rotation pole is found to drift at a mean linear rate of 3.901 ± 0.022 mas

per year (or ca. 12 cm per year at the surface) in the direction towards 65.17 ± 0.22^{o} West longitude. The cause of this westward secular polar motion is most likely post-glacial rebound (see, e.g., Nakiboglu and Lambeck 1980, Milne and Mitrovica 1998).

Concerning the low-frequency variations in polar motion, the prograde, retrograde and total amplitude spectra of the low-frequency part of polar motion from the POLE2001(JPL), EOP(IERS)C01, and OA00(AICAS) time series plotted in Fig. 9 show distinct peaks with periods at 9, 18 and 30 years. Especially for the 9-year and 18-year variations, both prograde and retrograde amplitudes reach ca. 6 mas, and the total amplitude (semi-major axis) ca. 11–13 mas. On the contrary, there is the 30-year signal with a retrograde amplitude of ca. 11 mas larger than the prograde amplitude of ca. 4 mas, while its total amplitude (semi-major axis) is ca. 15 mas. Markowitz was the first to report the existence of an oscillation in polar motion having a period of about 24 years (Markowitz 1960), hence, this wobble is referred to as the Markowitz wobble. Further studies aimed at estimating its parameters have been made; see, e.g., Wilson and Vicente (1980), Dickman (1981), Okamoto and Kikuchi (1983) and, for a review, Poma (2000). Compared to the previous estimates for the Markowitz wobble, our results re-confirm that there exists such a wobble with a period length of about 30 years, but smaller in its amplitude (semi-major axis) at a direction of about 15^{o} East longitude. For other peaks appearing in the amplitude spectra of Fig. 9, we can say that the corresponding signals should be rather unstable in both amplitude and period. Relative to this, the same assertion based on Fourier and wavelet spectra analysis can be found in Schuh et al. (2001). Long-term polar motion is probably caused by global mass redistributions in the atmosphere, hydrosphere and cryosphere, as well as geomagnetic and topographic core-mantle couplings and inner-core rotation being possible causes. For more information, see, e.g., Lambeck (1980), Eubanks (1993), Jochmann (1993), Greiner-Mai (1993), Greiner-Mai et al. (1999) and references therein.

Chandler wobble (Tables 6 and 8, Figures 3, 6, 10, 11, 14, 15, 18, 19 and 22, Appendix: Figures A1, B1 and B2)

In Figs. 3 and 6, we see similar curves of the Chandler terms of polar motion filtered out from the POLE2001(JPL), EOP(IERS)C01, OA00(AICAS), EOP(IERS)C04 and SPACE2001(JPL) time series in the x_1- and x_2-components over the common intervals. Concerning the temporal variability in amplitude, there are pronounced minima in 1921–1941 and 1965–1977 and maxima in 1909–1913, 1949–1955 and 1991–1993.

The Chandler wobble analysis includes about 89 cycles between 1893–1997. For the parameter variability of this periodic PM component, the curves plotted in Figs. 10, 11, 14, 15, 18 and 19 more clearly describe the characteristics and time evolution, rather than those in Figs. 3 and 6. Concerning the variability in radius of the Chandler wobble over time, plotted in Figs. 10 and 11, there is good agreement relative to the different PM systems, including different sampling. In particular, for all cycles over the 20th century, we can state the extreme radii (for the semi-major axis) as given in Table 8. Note that the smallest and biggest radii listed are the last lines. According to these results, the radius changes by up to ca. 240 mas. Obviously, there is a long-term motion course different for a decrease in radius over time from an increase in radius. If the motion course decreases in radius, then this occurs over about 16 to 17 years. However, if it increases in radius, then this occurs over about 24 to 26 years. For example, the smallest Chandler motion took place in 1926, while the largest motion elapsed in 1952. During the interval from 1926 to 1952, there exists a nearly continuous increase in radius; see Fig. 10.

Concerning the ellipticity of the Chandler wobble, we find that the differences between the extreme radii (for the semi-major and semi-minor axes, respectively) over a cycle are relatively small. For example, a motion cycle with a largest radial change of 30 mas obtained from the EOP(IERS)C01 time series is elapsed from 1938.65 to 1939.80. Here, the maximum radius is 79 mas, and the minimum radius 49 mas, and giving a numerical eccentricity $\epsilon = 0.78$. In case of the OA00(AICAS) results, the motion cycle from 28714.1 to 29130.7, i.e. from June 1937 to August 1938, has a maximum radius of 66 mas and a minimum radius of 46 mas, therefore a largest radial change of 20 mas, i.e., the numerical eccentricity computed is now: $\epsilon = 0.72$. In general, the ellipticity is smaller, i.e., as given in Table 6.

Next, we discuss the directions of the maximum and minimum radii for the Chandler wobble relative to the different PM systems. Comparing their estimates plotted in the panels of Figs. 14 and 15, we can see that the direction angles marked are widely spread, but clearly less, if the time sampling interval becomes shorter. The reason for this is that the Chandler wobble is a quasi-circular motion, and therefore the magnitude of the maximum and minimum radii can be determined rather well, but not so the direction relative to the sampling interval. For a better understanding of this fact, we computed the mean direction change of the radius for the different sampling intervals of the PM time series listed in Table 5. Finally, shown in Fig. 15, the direction angles are relatively reliable for one-day sampling. Over the period from 1965, they only vary between 0^{o} and 45^{o}, i.e., the Chandler wobble has been rather stationary in its elliptic motion in recent years.

In the case of the Chandler period, we extrapolated the period length found from the first and last sampling points for each cycle to a full 360^{o}-revolution. Plotted in Figs. 18 and 19, there are very good agreements between the variations in period derived from the different PM time series, except between 1925–1927. Without this exception, the Chandler

Table 8. Extreme radii of the Chandler wobble relative to the PM systems over the 20th century

PM system	POLE2001(JPL)		EOP(IERS)C01			OA00(AICAS)		EOP(IERS)C04		SPACE2001(JPL)	
Extreme	Date	Radius	Date		Radius	Date	Radius	Date	Radius	Date	Radius
N	(MJD)	(mas)	(year)	(MJD)	(mas)	(MJD)	(mas)	(MJD)	(mas)	(MJD)	(mas)
1	19087.9	228.26	1911.00	19037.0	232.81	19087.0	229.40				
2	24779.7	31.68	1926.25	24606.0	29.19	24840.5	12.88				
3	26575.5	71.00	1931.70	26598.0	80.62	26809.4	67.82				
4			1934.05	27456.0	63.09	27820.1	60.36				
5	28858.3	58.67	1937.95	28881.0	76.81						
6	34397.9	266.83	1952.40	34158.0	257.04	34179.9	261.10				
7	37959.1	146.47	1962.90	37994.0	151.00	37854.9	152.60				
8	38689.6	156.26	1964.80	38687.0	159.07						
9	40394.1	121.18	1968.90	40185.0	119.94	40234.9	125.97	40298.0	116.03		
10	45812.0	185.79	1984.30	45810.0	185.39	45650.0	183.89	45933.0	184.59	45809.0	186.50
11	46786.0	176.02	1986.95	46778.0	176.28			47134.0	172.51	47025.0	177.17
12	49251.4	200.64	1993.30	49098.0	202.98			49154.0	199.22	49256.0	200.12
Smallest		31.68			29.19		12.88		116.03		177.17
Biggest		266.83			257.04		261.10		199.22		200.12

period length varies between 410 and 442 days.

For further consideration, the same Chandler motion cycle chosen from the POLE2001(JPL), EOP (IERS)C01, OA00 (AICAS), EOP(IERS)C04 and SPACE2001(JPL) estimates (elapsed over the interval from May 1982 to July 1983) is presented in the upper part of Fig. 22. Moreover, see Fig. A1 in Appendix A for the motion cycles of the Chandler wobble over the total analysis intervals relative to the EOP(IERS)C04 and SPACE2001(JPL) systems, and, as mentioned above, Höpfner (2002a+d).

Annual wobble (Tables 6, 9 and 10, Figures 4, 7, 12, 13, 16, 17, 20, 21 and 22, Appendix: Figures A2, B1 and B2)

The annual terms of polar motion filtered out from the POLE2001(JPL), EOP(IERS)C01, OA00 (AICAS), EOP(IERS) C04 and SPACE2001(JPL) time series in the x_1- and x_2-components and shown in Figs. 4 and 7 are in good agreement over the common intervals. For the amplitude of both components, we notice that there exists a permanent change of larger to smaller amplitude values and vice versa. In particular, the minima appear in 1905, 1915, 1927, 1936, 1943, 1947, 1957, 1967, 1975 and 1981, and the maxima in 1902, 1910, 1923, 1932, 1939, 1945, 1953, 1961, 1973, 1977 and 1985.

The annual wobble is separated out from over 105 cycles in 1892–1997. As for the Chandler wobble, we look at the curves of the radii, directions and period lengths that are plotted in Figs. 4, 7, 12, 13, 16, 17, 20 and 21 in order to better discover the characteristics and time evolution of the annual wobble. Compared to the Chandler wobble, the change in the annual wobble radius over time plotted in Figs. 12 and 13 is smaller in magnitude and shorter in time. There appears to be a cyclic decrease then increase of ca. 20 to 40 mas every three to four years. The extreme radii (for the semi-major axis) are presented in Table 9, where the smallest and biggest radii are both listed in the last lines. For the annual wobble, the smallest motion cycle occurs in 1927, while the largest motion cycle is in 1953, with a radius change between the extreme radii of ca. 70 mas.

Relative to the different PM systems, the variability in the superior envelope of the radii of the change in semi-major axis is similar in its temporal course, but clearly different at times in magnitude. For example, the largest peak from the EOP(IERS)C01 system occurs in 1951–1953 with ca. 160 mas. Compared to this value, the same peaks for POLE2001(JPL) and OA00(AICAS) only show values of ca. 126 mas and ca. 135 mas, respectively. In all other cases, the distinctions are smaller, i.e. ca. 20 mas. Similarly to the variations in the superior envelope of the radii, similar variations arise in the inferior envelope of the change in semi-minor axis. However, there are again disagreement within the details, e. g., for the minimum in 1927 and the maximum in 1953. Also, it should be said that the inferior envelope of the radii for the OA00(AICAS) system (see the bottom panel of Fig. 12) appears smaller in magnitude than those for the POLE2001(JPL) and EOP(IERS)C01 systems from 1959 to 1989.

For the ellipticity of the annual wobble, it is to establish that the differences between the extreme radii (for the semi-major and semi-minor axes, respectively) over one cycle are ca. 10 to 20 mas for the POLE2001(JPL) system, but somewhat greater for the EOP(IERS)C01 and OA00(AICAS) systems, i.e., ca. 20 to 30 mas. Moreover, we can see a disagreement between the differences for the OA00(AICAS) system with those of the POLE2001(JPL) and EOP(IERS)C01 systems from 1959 to 1989, concurent with the OA00(AICAS) inferior envelope of the radii being smaller in magni-

Table 9. Extreme radii of the annual wobble relative to the PM systems over the 20th century

PM system	POLE2001(JPL)		EOP(IERS)C01			OA00(AICAS)		EOP(IERS)C04		SPACE2001(JPL)	
Extreme	Date	Radius	Date		Radius	Date	Radius	Date	Radius	Date	Radius
N	(MJD)	(mas)	(year)	(MJD)	(mas)	(MJD)	(mas)	(MJD)	(mas)	(MJD)	(mas)
1	18844.4	122.73	1910.55	18873.0	133.76	19087.0	120.01				
2	20122.7	104.24	1913.55	19969.0	106.40	20673.9	107.78				
3	21218.5	123.84	1916.40	21009.0	132.16	21695.5	117.05				
4	22618.6	99.16	1919.75	22233.0	103.36	22401.0	111.24				
5	23136.0	110.87	1922.65	23292.0	123.20	23305.2	118.95				
6	24871.0	69.96	1927.05	24899.0	82.26	25136.5	59.05				
7	26392.9	114.09	1931.10	26379.0	125.13	26386.8	117.11				
8	28066.9	94.77	1935.55	28004.0	83.49	28038.2	90.25				
9	28767.0	97.24	1939.10	29301.0	117.24	29311.2	110.61				
10	29984.5	87.35	1941.60	30214.0	94.91	30043.1	92.66				
11	30775.9	92.54									
12			1945.65	31693.0	109.83	31696.5	129.28				
13	32449.9	84.38	1947.65	32423.0	87.72	32784.6	106.51				
14	34124.0	125.66	1952.55	34213.0	160.29	34415.7	135.28				
15	35585.0	81.30	1956.55	35674.0	103.04	35698.4	88.85				
16			1959.60	36788.0	121.03						
17	37350.4	114.78				37529.8	117.51				
18	39389.7	85.04	1967.10	39528.0	93.08	38799.9	100.77				
19	40911.6	99.44	1971.65	41189.0	106.59	40984.9	105.00	40454.0	99.17		
20	41794.2	94.45	1974.20	42146.0	98.98	41714.9	103.33				
21	43042.2	113.25	1977.20	43217.0	116.52	42819.9	112.47	43047.0	117.13		
22	44472.7	75.07	1981.15	44660.0	66.51	44640.0	83.50	44675.0	79.71		
23	45964.2	97.87	1984.70	45956.0	103.74	45535.0	91.77	46133.0	95.84	46134.0	95.65
24	49038.4	58.30	1993.20	49061.0	55.42			49053.0	60.62	49053.0	60.51
Smallest		58.30			55.42		59.05		60.62		60.51
Biggest		125.66			160.29		129.28		117.13		95.65

Table 10. Numerical eccentricity ϵ computed for the same motion cycles of the annual wobble relative to the PM systems. Note: a, maximum of the radii (semi-major axis); b, minimum of the radii (semi-minor axis).

PM system		POLE2001(JPL)				EOP(IERS)C01				OA00(AICAS)			
N	Extreme a/b	Date (MJD)	Radius (mas)	a-b (mas)	ϵ	Date (year)	Radius (mas)	a-b (mas)	ϵ	Date (MJD)	Radius (mas)	a-b (mas)	ϵ
1	b	18753.0	102.23			1910.30	94.89			18991.8	90.63		
	a	18844.4	122.73	20.50	0.55	1910.55	133.76	38.87	0.70	19087.0	120.01	29.38	0.66
	b	18935.7	106.39	16.34	0.50	1910.80	98.59	35.17	0.68	19172.2	91.70	28.31	0.64
2	b	20031.4	86.22			1913.30	81.26			20593.4	100.78		
	a	20122.7	104.24	18.02	0.56	1913.55	106.40	25.14	0.65	20673.9	107.78	7.00	0.35
	b	20214.0	83.84	20.40	0.59	1913.80	82.94	23.46	0.63	20789.6	103.67	4.11	0.27
7	b	26301.5	105.66			1930.80	99.12			26279.8	95.90		
	a	26392.9	114.09	8.43	0.38	1931.10	125.13	26.01	0.61	26386.8	117.11	21.21	0.57
	b	26484.2	105.11	8.98	0.39	1931.35	98.86	26.27	0.61	26478.5	95.68	21.43	0.58
8	b	27975.6	85.66			1935.30	69.64			27946.9	73.92		
	a	28066.9	94.77	9.11	0.43	1935.55	83.49	13.85	0.55	28038.2	90.25	16.33	0.57
	b	28158.2	86.71	8.06	0.40	1935.80	73.21	10.28	0.48	28129.5	76.27	13.98	0.53
17	b	37259.1	95.59			1960.85	87.84			37439.8	77.38		
	a	37350.4	114.78	19.19	0.55	1961.10	115.93	28.09	0.65	37529.8	117.51	40.13	0.75
	b	37441.7	95.86	18.92	0.55	1961.35	86.64	29.29	0.66	37619.9	75.90	41.61	0.76
21	b	42950.9	102.60			1976.95	100.45			42724.9	83.89		
	a	43042.2	113.25	10.65	0.42	1977.20	116.52	16.07	0.51	42819.9	112.47	28.58	0.67
	b	43133.5	103.10	10.15	0.41	1977.45	101.03	15.49	0.50	42904.9	85.74	26.73	0.65
22	b	44411.9	70.62			1980.95	60.89			44550.0	62.12		
	a	44472.7	75.07	4.45	0.34	1981.15	66.51	5.62	0.40	44640.0	83.50	21.28	0.67
	b	44564.1	69.46	5.61	0.38	1981.40	62.80	3.71	0.33	44730.0	61.49	22.01	0.68
Range of ϵ				0.34 ... 0.59				0.33 ... 0.70				0.27 ... 0.76	

tude. For a numerical confirmation, we computed some values of the eccentricity ϵ for the same motion cycles of the annual wobble relative to the different PM systems. These and additional information are given in Table 10, where the examples, according to their numbers N, are identical with those listed in Table 9. Consequently, as can be seen relative to the PM systems, if the time sampling is shorter, then the ellipticity increases. Comparing the OA00(AICAS) results plotted in Fig. 12 with those of EOP(IERS)C04 plotted in Fig. 13 over the common intervals, we find that, in the case of OA00(AICAS), the motion cycles are too elliptic between 1959 and 1989.

A comparison of the directions of the maximum and minimum radii for the annual wobble found from each PM system as plotted in Figs. 16 and 17 shows that the orientation of the elliptic annual motion is obtained with more certainty, i.e., better than for the orientation of the little-elliptic (quasi-circular to oval) Chandler motion. Considering the mean direction change of the radius for the annual motion of each PM time series with different sampling intervals (Table 5), the temporal evolution of the maximum and minimum directions, while already reliably determined relative to the POLE2001(JPL) system with monthly sampling, is better resolved relative to the other PM systems with shorter sampling. The reason is that the annual motion is more elliptic than the Chandler motion. In particular, we find that the direction of the semi-major axis of the annual wobble lies between $138^o$and 195^o.

In order to obtain optimal period length estimates for the annual wobble, we computed the values by extrapolation relative to the full 360^o-revolution as made for the Chandler period lengths. As can be seen in Figs. 20 and 21, the curves of the variation in the annual period relative to the POLE2001(JPL), EOP(IERS)C01, OA00(AICAS), EOP(IERS)C04 and SPACE2001(JPL) systems are similar in detail over the common intervals, except for a disagreement between the OA00(AICAS) estimates to the others in 1927/1928. Consequently, the annual period ranges from 356 to 376 days over the 20th century.

As for the Chandler wobble, we show a selected motion cycle of the annual wobble relative to the five different PM systems, and all the motion cycles of the annual wobble over the total analysis intervals relative to the EOP(IERS)C04 and SPACE2001(JPL) systems. For the same annual motion cycle (elapsed over the interval from August 1984 to September 1985), see the lower part of Fig. 22, and for the pictures of all the motion cycles over the analysis intervals, see Fig. A2 (Appendix A). More details may be found in Höpfner (2002a+d).

Assessment of the results derived for the Chandler and annual wobbles

Finally, we now compare our results for the Chandler and annual wobbles with those found by other authors. Regarding our estimates, in each filtering of the Chandler and annual terms, the intervals used were about 5.2 and 4.3 years, respectively, being the same for the various PM time series with different time sampling intervals. See Table 2 for further details.

Using the PM time series of Fedorov et al. (1972), Nastula et al. (1993) showed the variations in the x-coordinate of the Chandler and annual wobbles of polar motion obtained by band-pass filtering, especially for two different bandwidths, in 1846–1988. Comparing our curves (Figs. 3 and 4, upper part) with these, we find an agreement to the Chandler and annual x-components filtered out using a band-pass filter with a broader bandwidth, i.e., 0.16 cycles per year (cpy). Furthermore, we can compare the envelopes of the observed Chandler and annual wobbles plotted there with our variations in the radii of Figs. 10 and 12. In the case of the Chandler results, a similarity is seen in time evolution, while there is disagreement in the magnitude, i.e., our (superior) envelope is smaller. In the case of the annual results, we notice that no good agreement exists, most likely because the amplitude variation of Nastula et al. (1993) is considerably smoothed.

From a variety of PM time series spanning different time periods from 1846 through to the early 1990s, Vicente and Wilson (1997) estimated the Chandler frequency. Their preferred estimate of the frequency is 0.8433 ± 0.003 cpy, or that of the period length 433.1 ± 1.7 days. Concerning the variability of the Chandler frequency, their conclusion is that, when associated intervals of confidence are considered, it is not significant. As our results plotted in Figs. 18 and 19 show, there exists a more substantial variation, and therefore, we can not confirm the Vicente and Wilson (1997) result.

Next, relative to the OA(AICAS) system, we compare our solutions with those obtained by Vondrák (1999) for the Chandler and annual wobbles using a least-squares fit with a running 8.5-year interval. For the semi-major and semi-minor axes of the Chandler wobble, we find similar curves in their temporal evolution, except for a disagreement in 1965. As can be seen in the bottom panel of Fig. 10, our curve has a small intermaximum at this time. By contrast, for the semi-major and semi-minor axes of the annual wobble, we notice that the curves of Vondrák (1999) are clearly smoother in their temporal variability than ours, which are plotted in the bottom panel of the Fig. 12.

Concerning the PM results derived separately for the x- and y-components by Liu et al. (2000), who used a new wavelet analysis technique applied to the EOP97(IERS)C01 time series, there are relatively good agreements to our solutions of the Chandler and annual wobbles over the common intervals in both magnitude and temporal evolution.

Based on the EOP(IERS)C01 and OA97(AICAS) time series, Schuh et al. (2000, 2001) studied the parameters of the Chandler and annual wobbles by means of a 13.76-year least-square fit sliding over the analysis intervals, each including ca. 15–30 iterations to obtain a sufficient convergence. Comparing their variations in the Chandler semi-major and semi-

minor axes with ours (plotted in the centre and bottom panels of Fig. 10), while there are similar curves, those of Schuh et al. (2000, 2001) appear smoother in the temporal evolution. Also, since the semi-major axes show a smaller difference from the semi-minor axes, there are smaller ellipticity values. For this, an example is that the small intermaximum is missing in 1965; compare with above. Concerning the Chandler period in magnitude and temporal evolution, the results well agree, with exceptions between 1925–1935 where our estimates show greater variability. For the variations in the semi-major and semi-minor axes of the annual wobble obtained from both analyses, we find considerable similarity, both in the magnitude and temporal course and also in the ellipticity. The same can be said for the variability in the annual period.

In assessing our results based on these comparisons, we summarize our findings as follows.
- Our solutions are derived from the different PM time series by using digital band-pass filters with the shortest filter (or analysis) intervals. Therefore, they have the least degree of smoothing where their temporal resolution is the same as that of the input data.
- Since all estimates are obtain using the same method, but with different time sampling of the input data, the differences between each other over common intervals show uncertainties relative to the different PM systems of a relatively small magnitude.
- For the purpose of a comparison, only some parameters for the Chandler and annual wobbles estimated from the other methods are available. For example, estimates of the period lengths are missing in Vondrák (1999) or those of the semi-major axes orientation in Schuh et al. (2000, 2001).
- It is likely that the quality of our results is considerably high, since those derived from other methods such as least-squares fitting or the wavelet analysis confirm ours in magnitude and temporal evolution. However, the other parameter variations used here for comparisons have a smoother form.

5 Summary and concluding remarks

In order to confirm the existence of the polar motion of the Earth by resolving variations in latitude, intensive efforts at several observatories were undertaken towards the end of the 19th century. Finally, in 1888, Küstner detected a real latitude variation at the Berlin Observatory. Afterwards, the problem of polar motion has raised considerable interest within the scientific community. From 1889, permanent latitude observations began at the observatories of Berlin, Potsdam, Prague and Strasbourg, and, from 1890, at further stations for studying polar motion. In 1899, the International Latitude Service (ILS) began systematic and continuous latitude observations at six observing sites in order to monitor polar motion. Since then, this international theme has continued with the scope of activities growing considerably.

Based on optical astrometry and, since the middle of the 1970s, precise space geodesy techniques, there is now polar motion data including diverse time series solutions from the mid-19th century to the present. Recently, several homogeneous PM time series with different time sampling over much or the 20th century have become available. In studying past polar motion, the characteristics and temporal evolution of the long-periodic variations are still uncertainly determined. Therefore, the problem of the main PM components is re-examined.

The objective of this study was to quantify better the parameters of the low-frequency terms and the Chandler and annual wobbles of polar motion in their temporal variability. For our purpose, we have used the following five PM time series:
- POLE2001(JPL), a combined Earth orientation series with monthly sampling from 1900.1 to 2002.0,
- EOP(IERS)C01, with 0.05-year sampling from 1890.0 to 2000.0,
- OA00(AICAS), with 5-day sampling from 1899.7 to 1992.0,
- EOP(IERS)C04, with one-day sampling from 1962.0 to 2002.4, and
- SPACE2001(JPL), with one-day sampling from 1976.7 to 2002.1.

To separate the main PM components from the original time series with different time sampling intervals, we applied a low-pass filter, a Chandler band-pass filter and an annual band-pass filter, each designed as a zero-phase digital filter for monthly, 0.05-year, 5-day and one-day sampling. Here, recursive band-pass filtering was used to derive optimal solutions for the Chandler and annual wobbles, since the response functions of both band-pass filters partially cover each other. The low-frequency, Chandler and annual terms filtered out from the PM time series are separate solutions in the x_1- and x_2-components at the attached sampling intervals.

Using a simple unweighted least-squares fit, the linear trends of the rotation pole were computed from the filtered low-frequency terms for the x_1- and x_2-components. Moreover, using a Fast Fourier Transform, the prograde, retrograde and total amplitude spectra of the low-frequency part of polar motion were determined to reveal the periodic signals contained within the low-frequency terms.

For the Chandler and annual wobbles in the polar coordinate system, we calculated the radii, their direction angles

and the period lengths for both wobbles from the filtered PM terms in the Cartesian coordinate system. Furthermore, we determined the maxima and minima of the radii for the semi-major and semi-minor axes, their directions and the numerical eccentricity.

Comparing the results derived from the five PM time series with each other and with other recent estimates, we assessed the characteristics of the low-frequency part of polar motion, and those of the Chandler and annual wobbles.

Concerning the drift of the Earth's rotation pole, we determined a mean linear rate of 3.901 ± 0.022 mas per year in the direction towards 65.17 ± 0.22^{o} West longitude. Concerning the low-frequency variations, our results re-confirm a wobble with a ca. 30-year period, but only ca. 15 mas in amplitude (semi-major axis) at a direction of ca. 15^{o} East longitude. Other signals, in particular those at 9 and 18 years are rather unstable in both amplitude and period.

For the Chandler and annual wobbles, the curves of the variations in the radii, of the direction courses of the radii and of the variation in the period clearly exhibit their characteristics and time evolution.

Concerning the long-term change in the radius of the Chandler wobble, we found that a decrease occurs over ca. 16–17 years, but an increase over ca. 24–26 years, reaching ca. 240 mas. Here, the ellipticity is relatively small. Relative to the monthly sampling, the maximum and minimum radii (for the semi-major and semi-minor axes, respectively) are well resolved in magnitude, but less so in direction. The shorter the sampling interval, the smaller the uncertainty becomes. In the case of the Chandler period, its lengths extrapolated from the first and last sampling points of the cycles are quite similar in their time evolution, i.e., consistent relative to the different PM systems. Except between 1925–1927, the variation in the Chandler period is between 410 and 442 days over the analysis intervals.

For the long-term change in annual wobble radius, there is a continuous change between decreasing and increasing of ca. 20–40 mas every three to four years. In the case of variations in the superior envelope of the radii (for the semi-major axis), we found agreement in the time evolution, but some times disagreement in magnitude between the different PM systems. The same can be seen for the variations in the inferior envelope of the radii (for the semi-minor axis). If the time sampling is shorter, then the ellipticity is somewhat larger. Especially for the OA00(AICAS) system from 1959 to 1989, the annual motion cycles are more elliptically obtained than otherwise what likely is not realistic. Unlike the Chandler motion, the orientation of the elliptic annual motion is more certainly determined at the different sampling intervals, originating in greater ellipticity. It varies between $138^{o}$and 195^{o}. Relative to the different PM systems, the period length of the annual wobble shows a similarity in the details over the common intervals, except for a disagreement in the OA00(AICAS) system in 1927/1928, ranging from 356 to 376 days.

Finally, it should be noted that each parameter estimated in this study for the Chandler and annual wobbles is available as a function of time. Here the extreme radii (for the semi-major and semi-minor axes, respectively) and their directions in the elliptic motion cycles are referred to actual time points. Compared with other recent results, our estimates have the least degree of smoothing and appear to be of high quality. They show very well the characteristics and time evolution over the period of the 20th century.

Acknowledgements. We are grateful to Richard S. Gross, JPL, Pasadena, California, USA and Daniel Gambis, Observatoire de Paris, Paris, France and Jan Vondrák, Astronomical Institute, Prague, Czech Republic for making the combined Earth orientation series available by anonymous ftp access. Kevin Fleming is acknowledged for his linguistic advice that helped to improve the quality of this paper.

Appendix A Time evolutions of the Chandler and annual wobbles of polar motion

Figures A1 and A2 show the time evolution of the Chandler and annual wobbles of polar motion for the EOP(IERS)C04 and SPACE2001(JPL) time series over the analysis intervals in terms of the revolution motions in consecutive pictures. Here, a full cycle is plotted in each picture, except in the first and last pictures relative to each PM time series. Note that, in each picture, the date given in MJD is the start of the curve and the arrow indicates the direction of the motion. For the date of the end of the curve, see the subsequent picture. In Fig. A1, the Chandler wobble is plotted in 31 panels. Figure A2 shows the annual wobble in 37 panels.

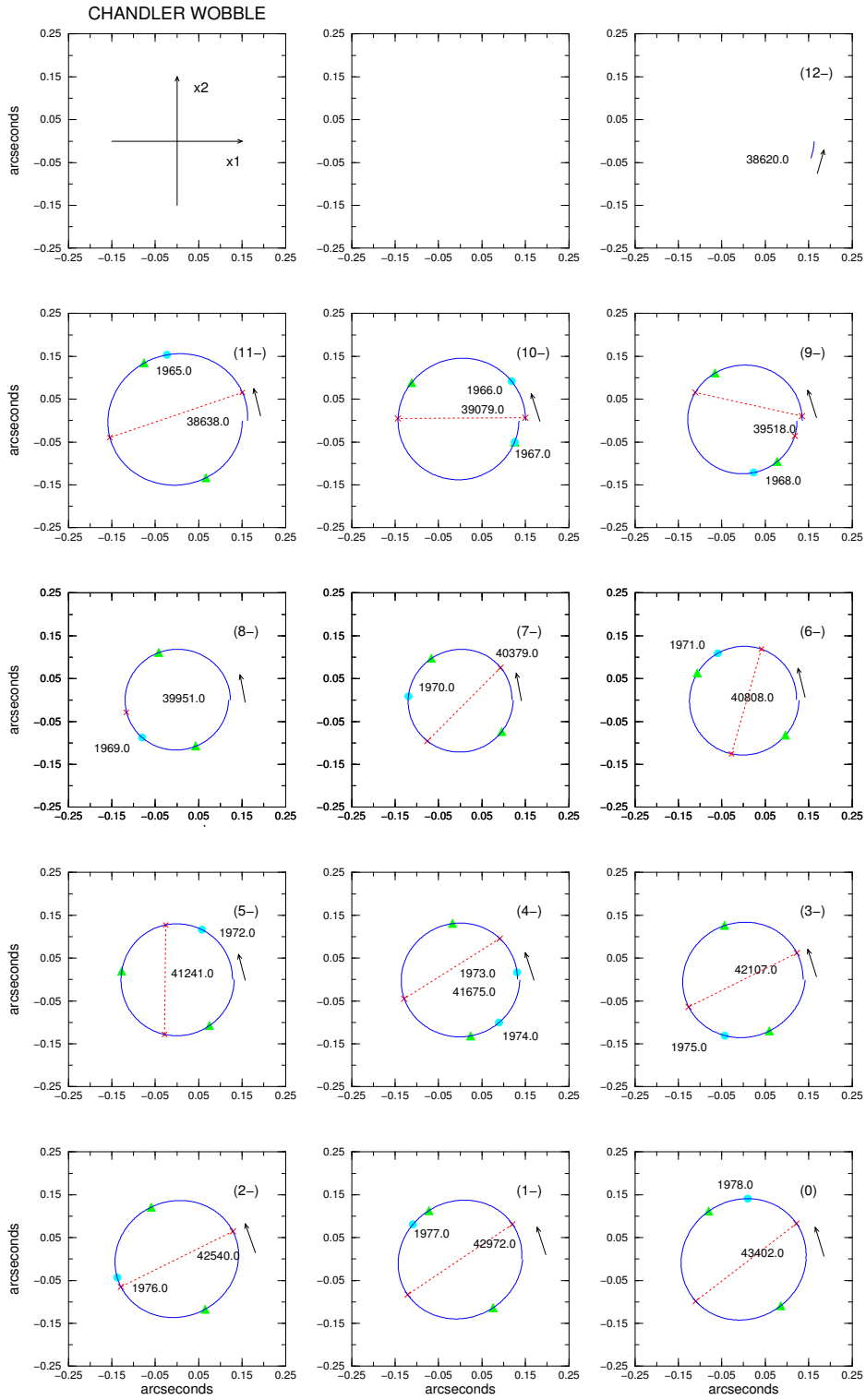

Figure A1. The Chandler wobble. The curves shown are the revolution motions over the analysis interval (from left to right and from top to bottom). The x_1-axis points towards the Greenwich meridian, and the x_2-axis towards 90°East longitude. The markers used are crosses in red at the maxima and triangles in green at the minima. Also indicated is the beginning of a year by a filled circle in cyan. Note that the EOP(IERS)C04 curves are plotted as solid lines in blue (in pictures (12-) to (18)) and the SPACE2001(JPL) curves as dotted lines in black (in pictures (1) to (18)). For their time intervals in calendar time, see Table 3.

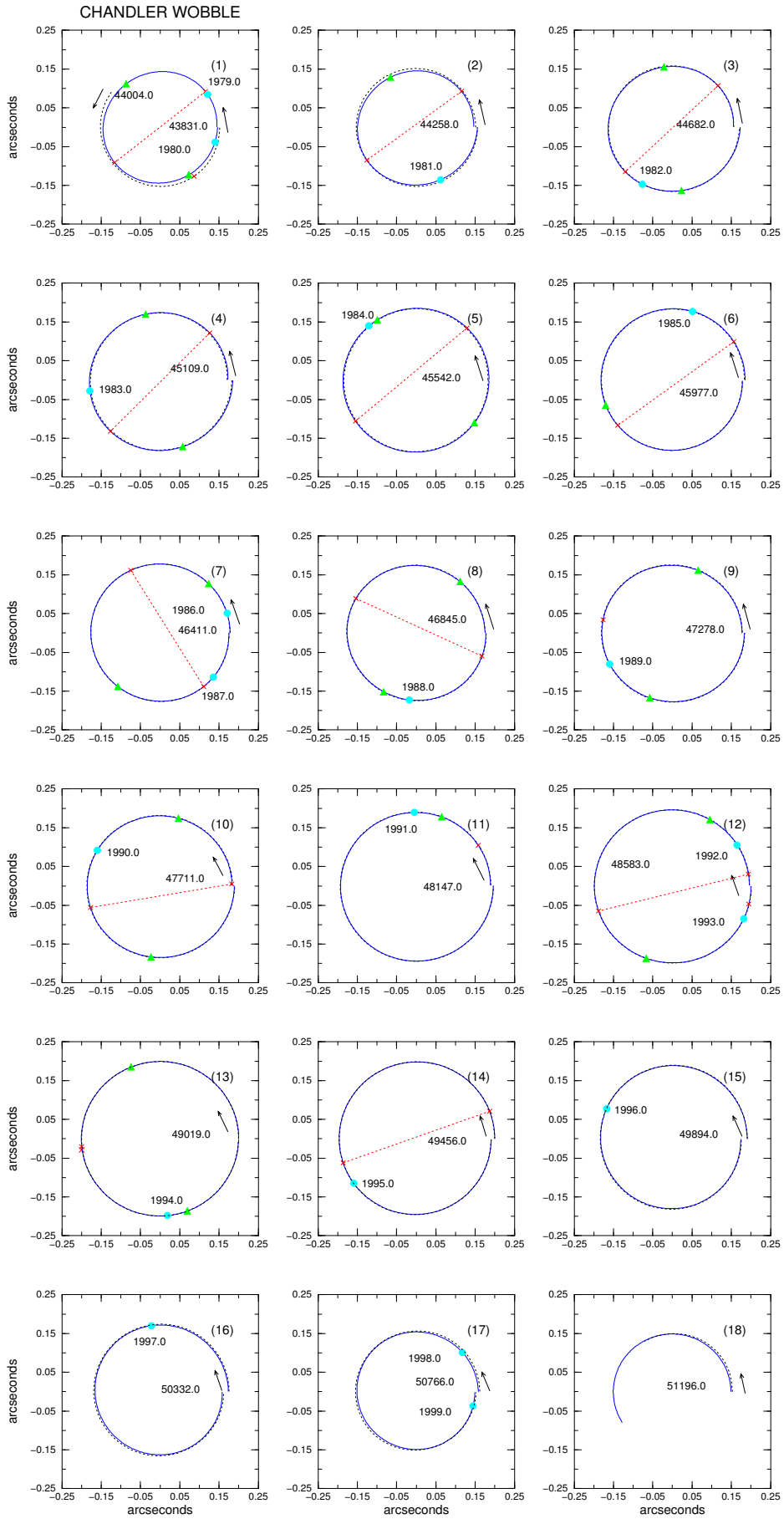

Figure A1. Continued

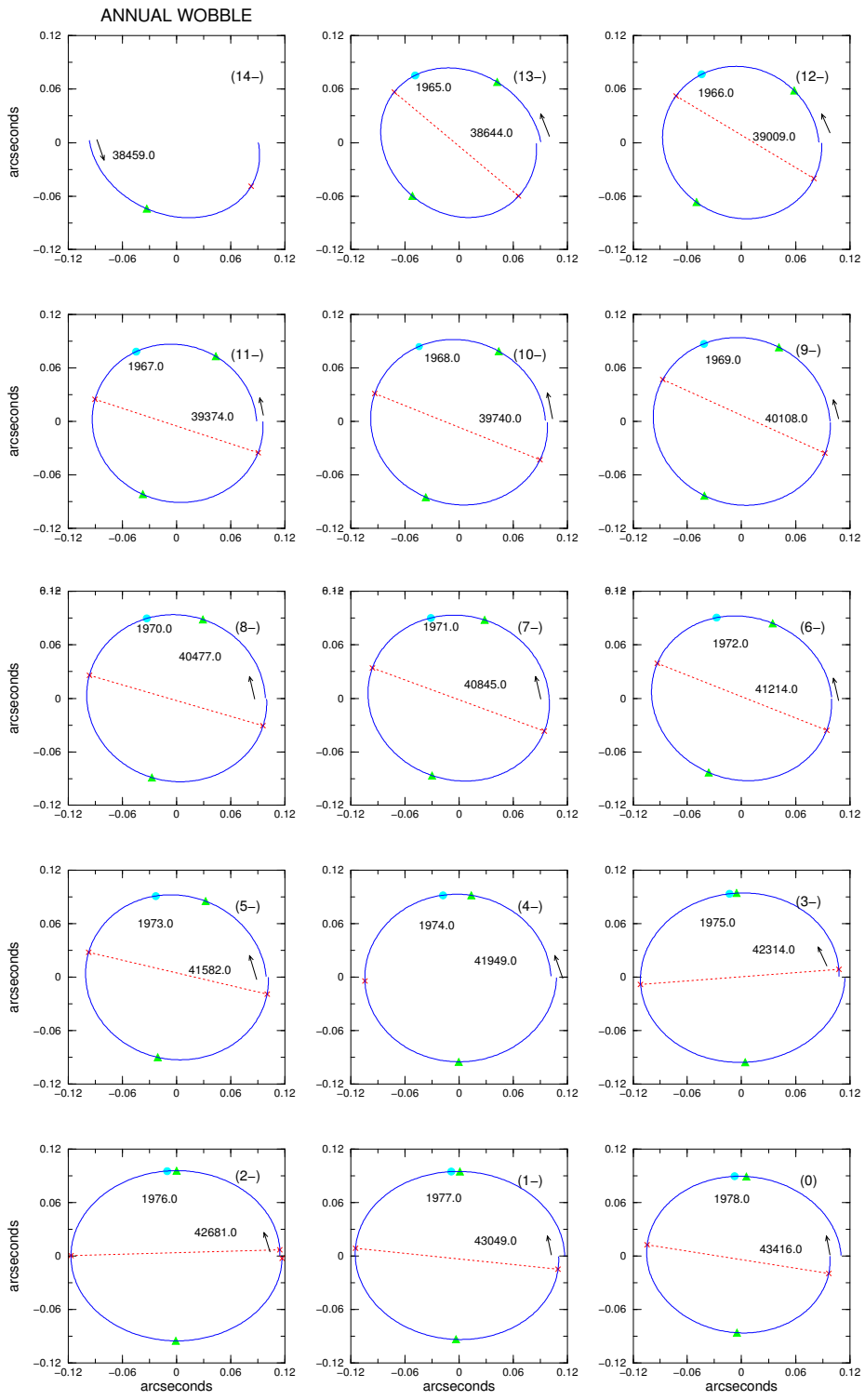

Figure A2. The annual wobble. The curves shown are the revolution motions over the analysis interval (from left to right and from top to bottom). The x_1-axis points towards the Greenwich meridian, and the x_2-axis towards 90°East longitude. The markers used are crosses in red at the maxima and triangles in green at the minima. Also indicated is the beginning of a year by a filled circle in cyan. Note that the EOP(IERS)C04 curves are plotted as solid lines in blue (in pictures (14-) to (22)) and the SPACE2001(JPL) curves as dotted lines in black (in pictures (1) to (22)). For their time intervals in calendar time, see Table 3.

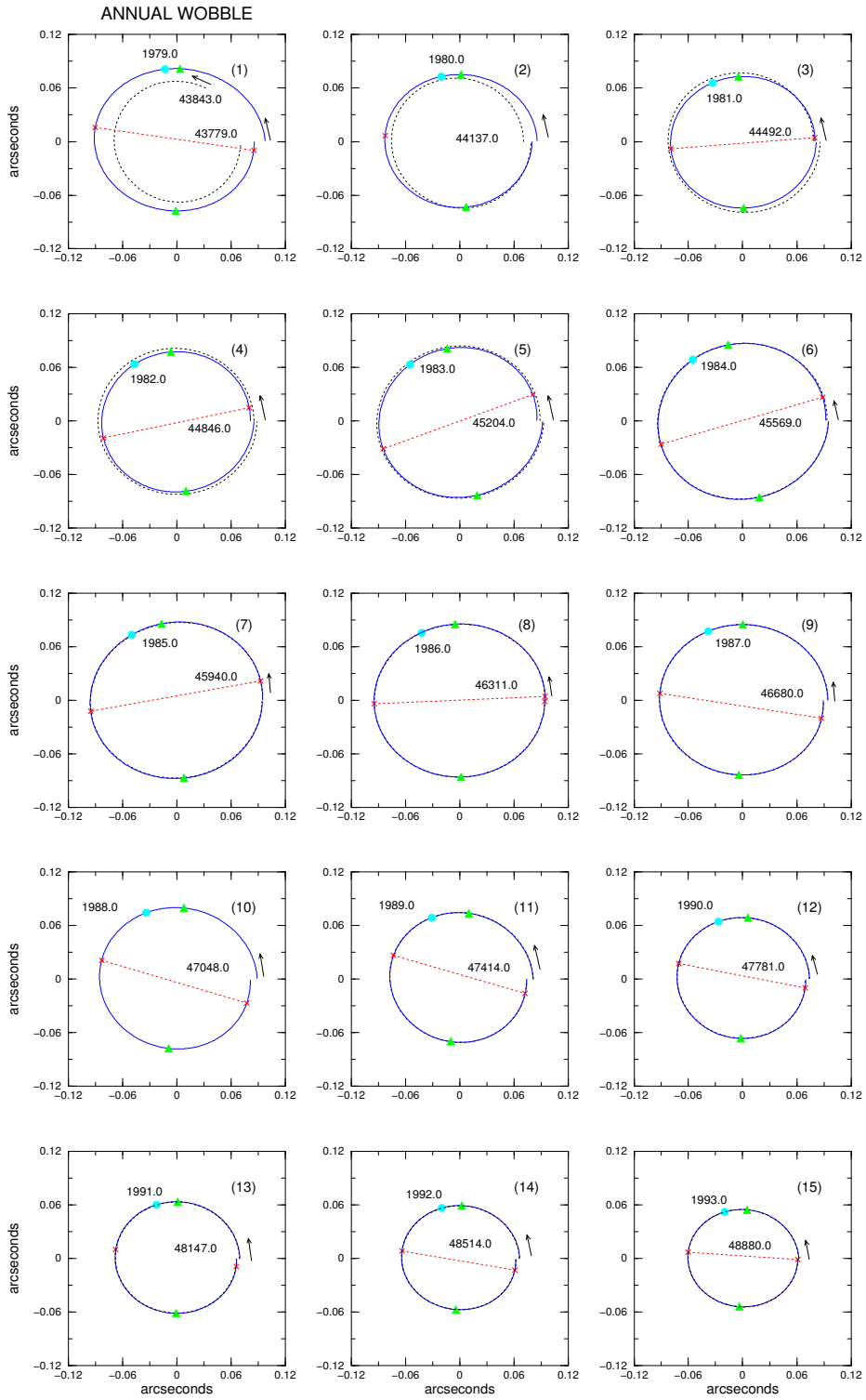

Figure A2. Continued

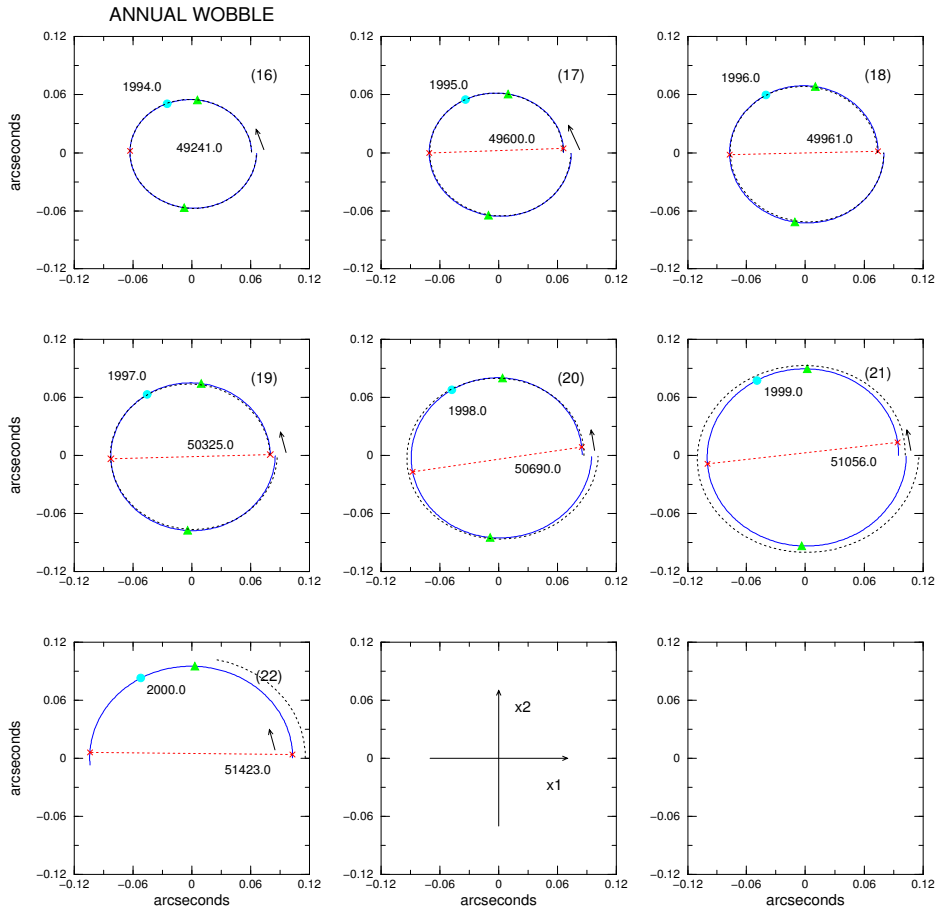

Figure A2. Continued

Appendix B Comparison of results obtained for the Potsdam Observatory

Based on the time series of the latitude changes obtained from observations made with a Danjon astrolabe at the Potsdam Geodetic-Astronomical Observatory between 1957.8 to 1978.0, the variability over time of mean latitude, Chandler, annual, semi-Chandler and semi-annual motions were studied (Höpfner 1983). We use these estimates of the periodic components for a comparison with those computed from the pole coordinates filtered out from the OA00(AICAS) and EOP(IERS)C04 time series in this study. Figure B1 shows the variations for the Chandler, annual, semi-Chandler and semi-annual motions as computed for the Potsdam Observatory. In Fig. B2, the variations in amplitude for the Chandler, annual, semi-Chandler and semi-annual motions at the Potsdam Observatory as computed from the pole coordinates are plotted together with those as observed with the Danjon astrolabe. Comparing these curves, we find that there is a good agreement between the results.

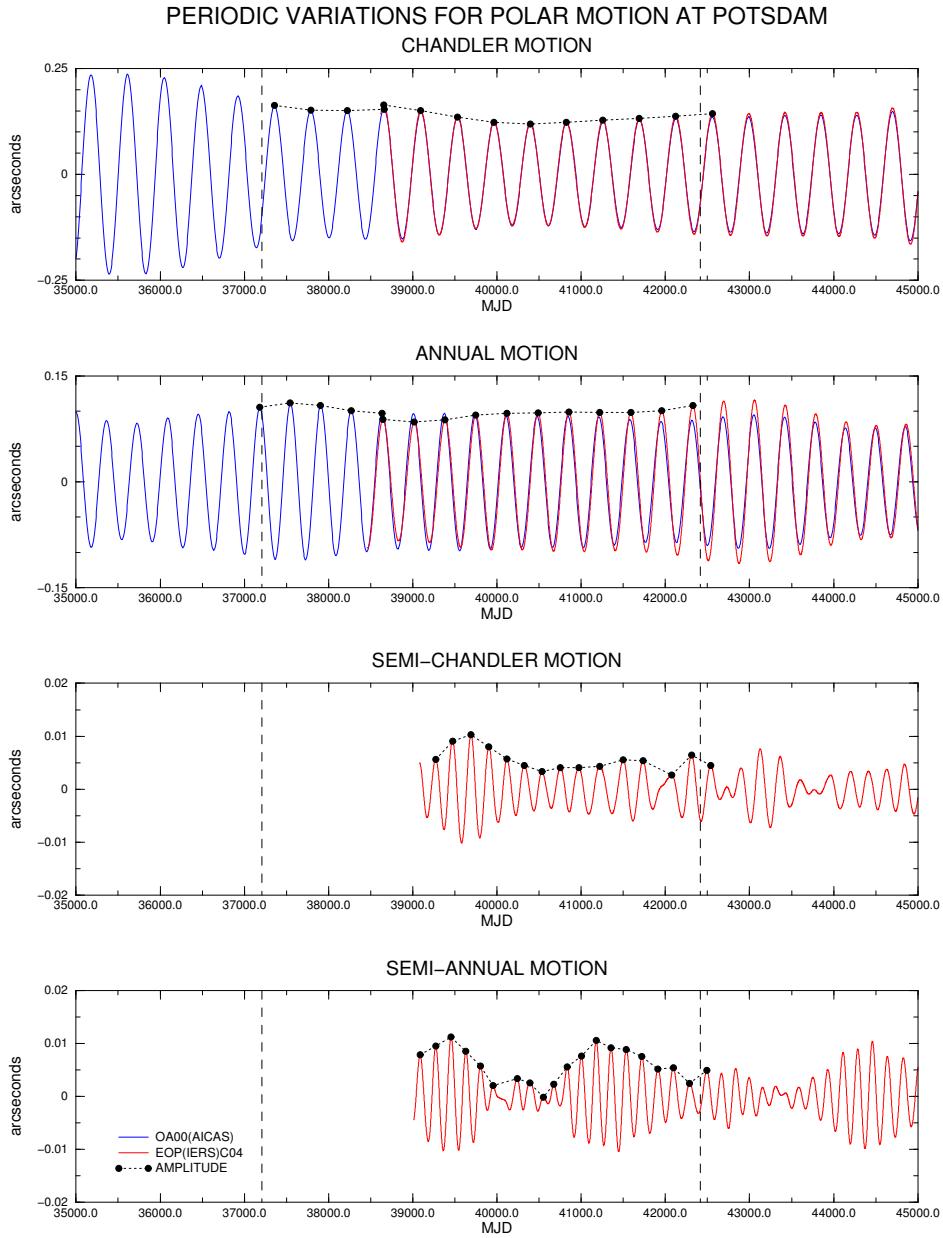

Figure B1. Periodic variations for polar motion at the Potsdam Observatory as computed from the OA00(AICAS) and EOP(IERS)C04 time series: Chandler, annual, semi-Chandler and semi-annual motions (from top to bottom). In each panel, the dotted curve with the filled circle markers is the variation in amplitude used for comparison.

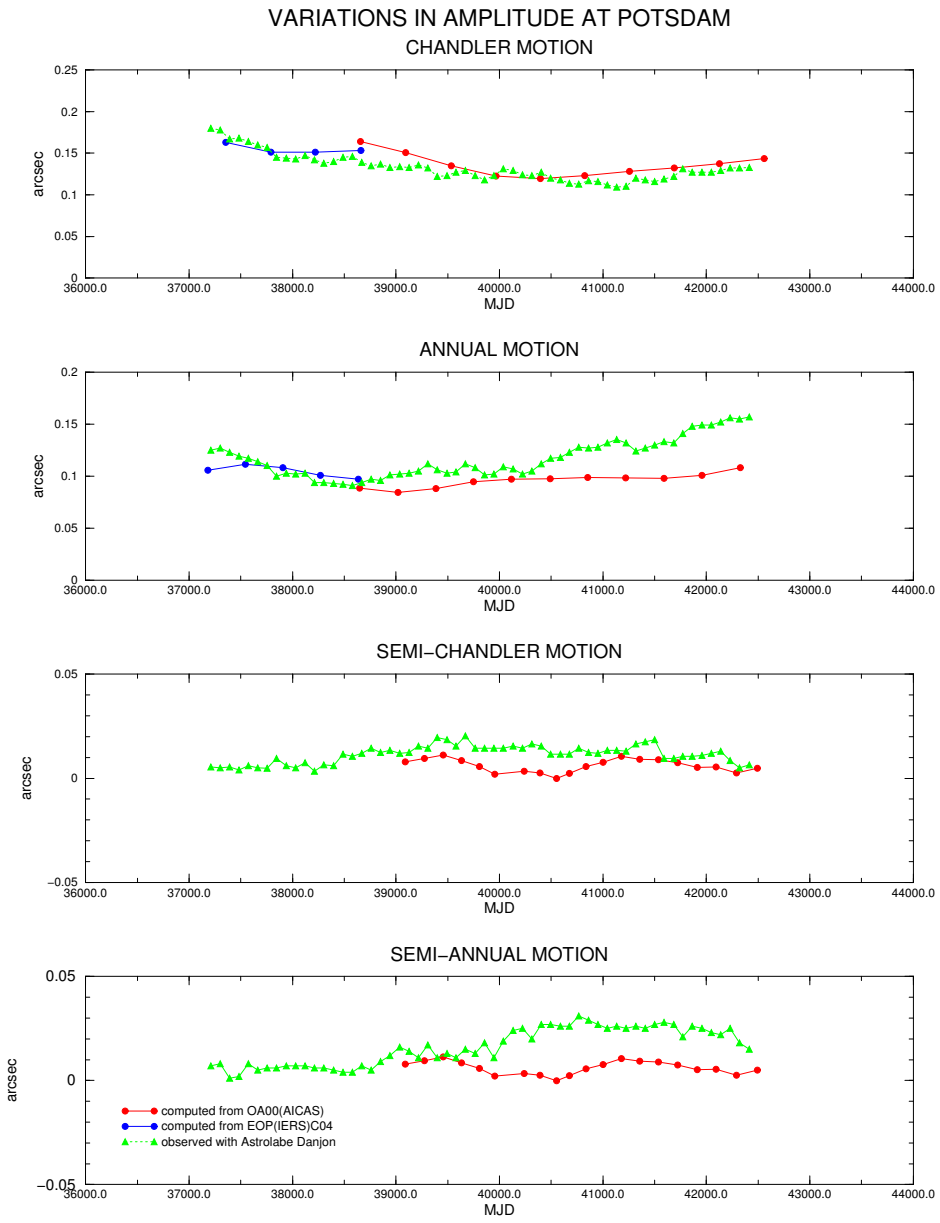

Figure B2. Comparison of variations in amplitude for the Chandler, annual, semi-Chandler and semi-annual motions (from top to bottom) as computed from the pole coordinates filtered out from the OA00(AICAS) and EOP(IERS)C04 time series and as observed with a Danjon astrolabe at the Potsdam Observatory. In each panel, the dotted curve with the filled circle markers is the variation in amplitude as computed and the solid curve with the filled triangle markers is that as observed.

References

Dick, S., McCarthy, D. and Luzum, B. (eds.), 2000. *Polar motion: Historical and scientific problems*. ASP Conf. Ser. Vol. 208. 641 pp.

Dickman, S. R., 1981. Investigation of controversial polar motion features using homogeneous International Latitude Service data. *J. Geophys. Res.. 86*, 4904–4912.

Eubanks, T.M., 1993. Variations in the orientation of the Earth. In: Smith, D.E. and Turcotte, D.L. (eds.), *Contributions of Space Geodesy to Geodynamics: Earth Dynamics*. AGU Geodyn. Ser. Vol. 24, 1–54.

Fedorov, E. P., Korsun, A. A., Mayor, S. P., Pantschenko, N. I., Tarady, V. K., Yatskiv, Ya. S., 1972. *Polar motion of the Earth from 1890.0 to 1969.0* (in Russian). Ukrainian Acad. Sc. Kiev.

Gambis, D., 2000. Long-term Earth orientation monitoring using various techniques. In: Dick, S., McCarthy, D. and Luzum, B. (eds.), *Polar motion: Historical and scientific problems*. ASP Conf. Ser. Vol. 208, 337–344.

Greiner-Mai, H., 1993. Decade variations of the Earth's rotation and geomagnetic core-mantle coupling. *J. Geomag. Geoelectr.*, *45*, 1333–1345.

Greiner-Mai, H., Jochmann, H. and Barthelmes, F., 1999. Influence of possible inner-core motions of the polar motion and the gravity field. *Phys. Earth Planet. Int.*, *117*, 81–93.

Gross, R. S., 2000. *Combinations of Earth Orientation Measurements: SPACE99, COMB99, and POLE99*. JPL Publication 00-5, Pasadena, California.

Gross, R.S. and Vondrák, J., 1999. Astrometric and space-geodetic observations of polar wander. *Geophys. Res. Lett.*, *26*, 2085–2088.

Höpfner, J., 1983. *Umfassende Analyse der Breitenbestimmungen des geodätisch-astronomischen Observatoriums Potsdam*. Diss. B. Techn. Univ. Dresden, 177 pp.

Höpfner, J., 2000. The International Latitude Service - a historical review, from the beginning to its foundation in 1899 and the period until 1922. *Surveys in Geophysics*, *21*, 5/6, 521–566.

Höpfner, J., 2001a. Chandler and annual wobbles based on space-geodetic measurements. Paper presented at the XXVI General Assembly, EGS, Nice, France, 26-30 March 2001. See Höpfner (2002a).

Höpfner, J., 2001b. Polar motions with periods of the order of a half-Chandler period and less in their temporal variability. Paper presented at the XXVI General Assembly, EGS, Nice, France, 26-30 March 2001. See Höpfner (2002b).

Höpfner, J., 2002a. Chandler and annual wobbles based on space-geodetic measurements. *Special Issue. J. Geodynamics* (in press).

Höpfner, J., 2002b. Polar motions with a half-Chandler period and less in their temporal variability. *Special Issue. J. Geodynamics* (in press).

Höpfner, J., 2002c. *Parameter variability of the observed polar motions with smaller amplitudes*. Scientific Technical Report STR 02/01. GFZ Potsdam, 35 p.

Höpfner, J., 2002d. Parameter variability of the observed Chandler and annual wobbles based on space-geodetic measurements. *ZfV*, *127*, 6, 397–408.

Höpfner, J., 2003. Parameter variability of the observed periodic oscillations of polar motion with smaller amplitudes. *J. Geodesy* (in press).

IERS, 2000. *1999 IERS Annual Report*. Central Bureau of IERS. Observatoire de Paris.

IERS, 2001. *2000 IERS Annual Report*. Central Bureau of IERS. Bundesamt für Kartographie und Geodäsie, Frankfurt am Main.

Jochmann, H., 1993. Earth rotation and global change. *Adv. Space Res.*, *13*, 271–280.

Kołaczek, B., Kosek, W., 1998. Variations of the amplitude of the Chandler oscillation. *Journées*, Paris, 215–221.

Kosek, W., Kołaczek, B., 1997. Semi-Chandler and semi-annual oscillations of polar motion. *Geophys. Res. Lett.*, *24*, 2235–2238.

Lambeck, K., 1980. *The Earth's variable rotation: Geophysical causes and consequences.* Cambridge University Press.

Li, Z., 1985. Earth rotation from optical astrometry, 1962.0–1982.0. In: BIH Annual Report for 1984, D31–D63. Obs. de Paris.

Li, Z. and Feissel, M., 1986. Determination of the Earth rotation parameters from optical astrometry observations, 1962.0–1982.0. *Bull. Géod.*, *60*, 15–28.

Liu, L.T., Hsu, H.T., Gao, B.X. and Wu, B., 2000. Wavelet analysis of the variable Chandler wobble. *Geophys. Res. Lett.*, *27*, 3001–3004.

Markowitz, W., 1960. Latitude and longitude, and the secular motion of the pole. In: Runcorn, S. K. (eds.), *Methods and Techniques in Geophysics*, Vol. I, Interscience, New York, 325–361.

Milne, G. A. and Mitrovica, J. X., 1998. Postglacial sea-level change on a rotating Earth. *Geophys. J. Int.*, *133*, 1–19.

Nakiboglu, S. M. and Lambeck, K., 1980. Deglaciation effects on the rotation of the Earth. *Geophys. J. R. Astr. Soc.*, *62*, 49–58.

Nastula, J., Korsun, A., Kołaczek, B., Kosek, W. and Hozakowski, W., 1993. Variations of the Chandler and annual wobbles of polar motion in 1846-1988 and their prediction. *Manuscripta Geodaetica*, *18*, 131–135.

Okamoto, I. and Kikuchi, N., 1983. Low frequency variations of homogeneous ILS polar motion data. *Publ. Int. Latit.. Obs. Mizusawa*, *16*, 35–40.

Poma, A., 2000. The Markowitz wobble. In: Dick, S., McCarthy, D. and Luzum, B. (eds.), *Polar motion: Historical and scientific problems*. ASP Conf. Ser. Vol. 208, 351–354.

Schuh, H., Richter, B. and Nagel, S., 2000. Analysis of long term series of polar motion. In: Dick, S., McCarthy, D. and Luzum, B. (eds.), *Polar motion: Historical and scientific problems*. ASP Conf. Ser. Vol. 208, 321–331.

Schuh, H., Nagel, S. and Seitz, T., 2001. Linear drift and periodic variations observed in long term series of polar motion. *J. Geodesy*, *74*, 701–710.

Yatskiv, Ya., 2000. Chandler motion observations. In: Dick, S., McCarthy, D. and Luzum, B. (eds.), *Polar motion: Historical and scientific problems*. ASP Conf. Ser. Vol. 208, 383–395.

Yumi, S. and Yokoyama, K., 1980. *Results of the ILS in a homogeneous system 1899.9–1979.0.* Publ. Central Bureau of the International Earth Rotation Service. Internat. Latitude Observ., Mizusawa. Japan. 199 pp.

Vicente, R. O. and Wilson, C. R., 1997. On the variability of the Chandler frequency. *J. Geophys. Res.*, *102*, B9, 20439–20445.

Vicente, R. O. and Wilson, C. R., 2002. On long-period polar motion. *J. Geodesy*, *76*, 199–208.

Vondrák, J., 1999. Earth rotation parameters 1899.7-1992.0 after reanalysis within the Hipparcos frame. *Surveys in Geophysics*, *20*, 169–195.

Vondrák J., Ron C., Pesek I., Cepek A., 1995. New global solution of Earth orientation parameters from optical astrometry in 1900-1990. *Astron. Astrophys.*, *297*, 899–906.

Vondrák, J., Pešek, I., Ron, C., and Čepek, A., 1998. *Earth orientation parameters 1899.7-1992.0 in the ICRS based on the Hipparcos reference frame*. Publ. Astron. Inst. Acad. Sc. Czech Rep. 56 pp.

Vondrák, J. and Ron, C., 2000. Survey of observational techniques and Hipparcos reanalysis. In: Dick, S., McCarthy, D. and Luzum, B. (eds.), *Polar motion: Historical and scientific problems*. ASP Conf. Ser. Vol. 208, 239–250.

Wilson, C. R. and Vicente, R. O., 1980. An analysis of the homogeneous ILS polar motion series. *Geophys. J. Roy. astr. Soc.*, *62*, 605–616.